ABCC9 knockdown attenuates isoproterenol-induced myocardial hypertrophy by inhibiting the PI3K/AKT signaling pathway

QIAN PENG[1], RUI CHANG[2], LINLIN MA[2] and YANFEI LI[2,3]

[1]Graduate School, Shanghai University of Traditional Chinese Medicine, Shanghai 201203, P.R. China; [2]Department of Scientific Research, Shanghai University of Medicine and Health Sciences Affiliated Zhoupu Hospital, Shanghai 201318, P.R. China; [3]Shanghai University of Traditional Chinese Medicine, Shanghai 201203, P.R. China

Received June 27, 2025; Accepted November 12, 2025

DOI: 10.3892/mmr.2025.13770

Abstract. Myocardial hypertrophy (MH) represents an early pathological manifestation that progresses to severe cardiovascular disease (CVD), and its reversal is important for preventing and treating heart failure. Dysregulated expression of ATP-binding cassette subfamily C member 9 (ABCC9) has been associated with complex CVD pathogenesis, although its precise mechanistic role remains ambiguous. The present study was designed to investigate the protective effects of ABCC9 knockdown against isoproterenol (ISO)-induced MH and elucidate its underlying molecular mechanisms. AC16 cardiomyocytes were treated with ISO to establish an MH model, in which ABCC9 protein expression was significantly elevated. Fluorescence staining of cardiomyocyte surface area and quantification of MH-related biomarkers, including atrial natriuretic peptide, brain natriuretic peptide and β-myosin heavy chain, demonstrated that ABCC9 knockdown effectively attenuated MH and improved cardiac function. Furthermore, western blot analysis and flow cytometry revealed that ABCC9 knockdown not only decreased cardiomyocyte apoptosis but also reduced oxidative stress, as indicated by lower reactive oxygen species levels. Mechanistically, western blotting and mitochondrial membrane potential assays showed that ABCC9 knockdown inhibited the phosphatidylinositol 3-kinase/protein kinase B (PI3K/AKT) signaling pathway and improved mitochondrial function. Notably, these protective effects were diminished by treatment with the PI3K/AKT activator 740Y-P. These findings collectively suggest that ABCC9 knockdown protects against MH by inhibiting the PI3K/AKT signaling pathway, thereby alleviating mitochondrial dysfunction and reducing apoptosis and oxidative stress, positioning ABCC9 as a potential therapeutic target for MH treatment.

Correspondence to: Professor Yanfei Li, Department of Scientific Research, Shanghai University of Medicine and Health Sciences Affiliated Zhoupu Hospital, 1500 Zhouyuan Road, Pudong New Area, Shanghai 201318, P.R. China
E-mail: liyf@sumhs.edu.cn

Key words: ATP-binding cassette transporter protein, ATP-binding cassette subfamily C member 9, isoproterenol, myocardial hypertrophy, PI3K/AKT signaling pathway

Introduction

Cardiovascular disease (CVD) is recognized as one of the leading causes of global morbidity and mortality (1,2), with its associated disease burden posing a substantial public health challenge. As reported by the American Heart Association, CVD is responsible for 32.9% of global non-communicable disease mortality, accounting for ~18 million deaths per year (3). CVD comprises a spectrum of pathological conditions, including coronary artery disease, myocardial hypertrophy (MH), hypertension, heart failure (HF) and peripheral artery disease (4,5). The prevalence of CVD has been steadily increasing, driven by population aging, the rising incidence of metabolic disorders and lifestyle modifications, leading to a marked escalation in socioeconomic burden (6).

MH serves an important role in the pathological progression of CVD and serves as a key etiological factor in numerous severe cardiovascular complications (7). As a compensatory pathological adaptation, MH is primarily characterized by cardiomyocyte responses to mechanical stress or neurohumoral stimuli, which sustain cardiac output and function (8). This pathological remodeling is typically triggered by chronic pressure overload, such as hypertension, or volume overload, such as valvular regurgitation (9). Notably, pathological cardiac hypertrophy has been identified as a notable contributor to HF (10), resulting in elevated global mortality rates. Consequently, an in-depth investigation of the molecular mechanisms underlying pathological cardiac hypertrophy is important for the prevention or reversal of HF.

Accumulating evidence indicates that the phosphatidylinositol 3-kinase (PI3K)/protein kinase B (AKT) signaling cascade is closely associated with MH (11-13). The PI3K/AKT pathway not only regulates fundamental biological processes, including cell migration, protein translation and cell survival, but also modulates energy metabolism, vascular homeostasis and thrombosis (14). In cardiomyocytes, dysregulated activation of this pathway can markedly influence the progression of MH (15), rendering it a key therapeutic target in CVD research. Matairesinol has been shown to attenuate stress-induced MH by upregulating peroxiredoxin-1 expression and suppressing

the PI3K/AKT/forkhead box protein O1 (FoxO1) axis (16). Similarly, astragaloside IV, a bioactive compound derived from Traditional Chinese Medicine, has been reported to inhibit cardiac hypertrophy by blocking TANK-binding kinase 1/PI3K/AKT signaling (17). Furthermore, a study reported by Qian *et al* (18) demonstrated that hanhuangqin significantly alleviated isoproterenol (ISO)-induced MH both *in vivo* and *in vitro* by inhibiting the PI3K/AKT hypertrophic pathway. Thus, downregulation of PI3K/AKT signaling may represent a promising therapeutic strategy.

ATP-binding cassette (ABC) subfamily C member 9 (ABCC9), an ABC transporter protein (19), is expressed in cardiac tissues, suggesting its potential involvement in cardiac drug responses or physiological processes. In cardiomyocytes, ABCC9 encodes sulfonylurea receptor (SUR) 2A, an 'atypical' ABC transporter protein (20). Despite sharing structural features with typical ABC proteins, SUR2A does not function as a transporter; instead, it serves as a regulatory subunit that binds to the inwardly rectifying potassium channel Kir6.2 (KCNJ11) (21). Together, SUR2A and KCNJ11 form ATP-sensitive potassium channels (KATP) in the ventricular myocyte membrane (22). The physiological functions of KATP channels are complex. It was found that although SUR2 deficiency causes vasospasm and increases the risk of sudden death, it also enhances the resistance of cardiomyocytes to ischemic injury (23). Additionally, Fahrenbach *et al* (24) demonstrated that ABCC9/SUR2A is important for the transition of the neonatal heart from fetal glycolytic metabolism to mature oxidative metabolism. Furthermore, SUR2A has been implicated in regulating myocardial resistance to metabolic and oxidative stress, as well as cardiac senescence (25).

Cantu syndrome (CS), a complex disorder caused by gain-of-function mutations in ABCC9 and ATP-sensitive inward rectifier potassium channel 8 (26,27), is characterized by cardiovascular abnormalities, including vasodilation (28), cardiac hypertrophy and other structural or functional defects (29). Currently, no targeted therapy exists for CS, and the reversibility of its cardiovascular manifestations remains ambiguous. Although ABCC9 has been implicated as a potential regulator of MH (30), its precise mechanistic role remains undetermined. Specifically, whether ABCC9 modulates ISO-induced MH and the underlying molecular pathways requires further investigation.

The present study aimed to examine the expression level of ABCC9 in ISO-induced hypertrophic AC16 cardiomyocytes and evaluate the biological effects of ABCC9 knockdown. Furthermore, the present study sought to determine whether ABCC9 silencing attenuated MH and improved cardiac function by suppressing the PI3K/AKT signaling axis, thereby proposing a novel therapeutic approach for ISO-induced MH.

Materials and methods

Chemicals and reagents. ISO hydrochloride (cat. no. HY-B0468) was purchased from MedChemExpress. The Color Reverse Transcription Kit (with gDNA Remover) (cat. no. A0010CGQ) and the 2x Color SYBR Green qPCR Master Mix (ROX2; cat. no. A0012-R2) used for qRT-PCR were purchased from EZBioscience. An anti-ABCC9 antibody (cat. no. 40229) was purchased from Signalway Antibody LLC. Antibodies against B-cell lymphoma 2 protein (Bcl-2; cat. no. 15071T), Bcl-2-associated X protein (Bax; cat. no. 2772T), caspase-3 (cat. no. 9662S), cleaved caspase-3 (cat. no. 9661S), phosphorylated (p)-PI3K (cat. no. 17366T), PI3K (cat. no. 4292S), p-AKT (cat. no. 9271T), AKT (cat. no. 4691T) and β-actin (cat. no. 3700S) were purchased from Cell Signaling Technology, Inc. Atrial natriuretic peptide (ANP; cat. no. ab189921) and brain natriuretic peptide (BNP; cat. no. ab236101) were purchased from Abcam. GAPDH (cat. no. sc-32233) and secondary antibodies were purchased from Santa Cruz Biotechnology, Inc., including mouse anti-rabbit IgG-HRP (cat. no. sc-2357) and mouse IgGκ light chain binding protein conjugated to HRP (cat. no. sc-516102). Necessary experimental materials, including PVDF membrane, RIPA buffer, Actin-Tracker Red-594 (a microfilament red fluorescent probe), 2'-7'-dichlorodihydrofluorescein diacetate (DCFH-DA), DAPI staining solution, mitochondrial membrane potential (MMP) assay kit with JC-1 and BCA protein detection kit were purchased from Beyotime Biotechnology. Annexin V-FITC/PI apoptosis detection kit was purchased from Shanghai Yeasen Biotechnology Co., Ltd. iF488-Wheat Germ Agglutinin (WGA; a green fluorescent dye) was purchased from Wuhan Servicebio Technology Co., Ltd. 740Y-P (PI3K/AKT activator; cat. no. HY-P0175) was purchased from MedChemExpress.

Cell culture. The immortalized human cardiomyocyte AC16 cell line was purchased from Ningbo Mingzhou Biotechnology Co., Ltd. (cat. no. MZ-4038), and the cells were cultured in DMEM (Shanghai Basal Media Technologies Co., Ltd.) high-dextran culture medium supplemented with 10% fetal bovine serum (Vazyme Biotech Co., Ltd.) and 1% penicillin/streptomycin solution (Shanghai Epizyme Biomedical Technology Co., Ltd.) at 37˚C, with a carbon dioxide concentration of 5%, in an incubator. Upon reaching logarithmic growth phase, cells were seeded into 6-well plates at uniform density and allowed to adhere for 24 h prior to experimental treatments.

Small interfering RNA (siRNA)-mediated gene silencing. The ABCC9-targeting siRNA (si-ABCC9) and the negative control (si-NC) were designed and synthesized by Suzhou Synbio Technologies Co., Ltd. Silencing of the ABCC9 gene in AC16 cells was accomplished by the use of Lipofectamine® 3000 (Invitrogen; Thermo Fisher Scientific, Inc.), a process that resulted in a notable downregulation of gene expression. When cells were grown to ~50% confluence, 5 μl Lipofectamine® 3000 and 50 nM siRNA were diluted separately using 125 μl Opti-MEM (Gibco; Thermo Fisher Scientific, Inc.). After 15 min of incubation at room temperature, the mixtures were combined. Concurrently, culture medium was replaced with fresh medium to maintain optimal cell health during transfection. The prepared siRNA-Lipofectamine® 3000 complexes were then added to cells in 6-well plates. Following a 24 h incubation at 37˚C with 5% CO_2, transfection efficiency was assessed using western blotting, and all subsequent experiments were performed 24 h after transfection. The oligo sequences used for RNA interference (shown in the 5'-3' direction) were as follows: ABCC9 siRNA-1, sense GGUCAG AUUUGCAGUCAAATT, antisense UUUGACUGCAAA

UCUGACCTT; ABCC9 siRNA-2, sense CAACGAUGGUGU ACUACAATT, antisense UUGUAGUACACCAUCGUUGTT; ABCC9 siRNA-3, sense GCGUGAUUCUGCUCUAUAATT, antisense UUAUAGAGCAGAAUCACGCTT; and si-NC, sense GCGACGAUCUGCCUAAGAUTT, antisense AUC UUAGGCAGAUCGUCGCTT.

Cell viability assay. AC16 cell viability was determined using the Cell Counting Kit-8 (CCK-8; Beyotime Biotechnology) assay according to the manufacturer's instructions. Briefly, cells (5,000 cells/well) were cultured in 96-well culture plates overnight at 37˚C and treated with different concentrations of ISO (0, 5, 10, 20 and 40 μmol/l) for 24 h. Subsequently, cells were rinsed once with phosphate-buffered saline (PBS), 10 μl CCK-8 solution was added to each well and cells were incubated at 37˚C for 2 h. Finally, the absorbance of each well was measured at 450 nm using a microplate reader (PT-3502PC; Bio-Equip.com). A line graph of optical density (OD) vs. ISO concentration was plotted, the experiment was repeated three times and cell viability was calculated as follows: Cell viability=(treated OD value-blank OD value)/(control OD value-blank OD value) x100.

Reverse transcription-quantitative PCR (RT-qPCR). Total RNA was extracted using TRIzol® reagent (Invitrogen; Thermo Fisher Scientific, Inc.) and RNA concentration was quantified using a NanoDrop® spectrophotometer (Thermo Fisher Scientific, Inc.). cDNA synthesis was carried out using the Color Reverse Transcription Kit (with gDNA Remover) (cat. no. A0010CGQ; EZBioscience) with the following thermal profile: 42˚C for 15 min followed by 85˚C for 5 sec. Subsequently, qPCR was performed on a Roche LightCycler®96 Real-time Quantitative Fluorescence PCR instrument using the 2x Color SYBR Green qPCR Master Mix (ROX2; cat. no. A0012-R2; EZBioscience) under the following conditions: Initial denaturation at 95˚C for 5 min, followed by denaturation at 95˚C for 30 sec, annealing at 58˚C for 30 sec and extension at 72˚C for 30 sec; a total of 40 cycles were performed. The primer sequences were as follows: ANP, forward 5'-CAACGCAGACCTGATGGATTT-3', reverse 5'-AGCCCCCGCTTCTTCATTC-3; BNP, forward 5'-TGGA AACGTCCGGGTTACAG-3', reverse 5'-CTGATCCGGTCC ATCTTCCT-3'; β-myosin heavy chain (β-MHC), forward 5'-TCACCAACAACCCCTACGATT-3', reverse 5'-CTCCTC AGCGTCATCAATGGA-3'; and β-actin, forward 5'-CAC CATTGGCAATGAGCGGTTC-3', reverse 5'-AGGTCTTTG CGGATGTCCACGT-3'. The $2^{-\Delta\Delta Cq}$ method (31) was used to assess mRNA expression levels.

Western blot analysis. After treatment as described previously (ISO 10 μM; 24 h; si-ABCC9 50 nmol/l; 24 h; 740Y-P 10 μM; 24 h; 37˚C), cells from each experimental group (Control; ISO; ISO + si-NC; ISO + si-ABCC9; ISO + si-ABCC9 + 740Y-P; ISO + 740Y-P) were washed three times with cold PBS and lysed for 30 min in RIPA buffer (cat. no. P0013C; Beyotime Biotechnology) supplemented with a protease and phosphatase inhibitor cocktail (50X; cat. no. P1045; Beyotime Biotechnology). The mixture was centrifuged at 12,000 x g for 30 min at 4˚C, and the supernatant protein concentration was measured using the BCA Protein Quantification Kit (cat. no. P0009; Beyotime Biotechnology). Equal amounts of proteins (30 μg per lane) were separated by 10% SDS-PAGE and transferred onto PVDF membranes. The membranes were blocked with 5% non-fat dry milk for 1 h at room temperature and subsequently incubated overnight at 4˚C with the following antibodies: ABCC9 (1:1,000), ANP (1:1,000), BNP (1:1,000), Bax (1:1,000), Bcl-2 (1:1,000), Caspase-3 (1:1,000), p-PI3K (1:1,000), PI3K (1:1,000), p-AKT (1:1,000), AKT (1:1,000), GAPDH (1:5,000) and β-actin (1:5,000). Subsequently, after washing with TBST (0.1% Tween-20), membranes were incubated with anti-rabbit (1:50,000) and anti-mouse (1:50,000) secondary antibodies for 1 h at room temperature. After washing again, protein bands were visualized using BeyoECL Moon chemiluminescent substrate (cat. no. P0018FS; Beyotime Biotechnology) and imaged with a Tanon-4600 chemiluminescence system (Tanon Science and Technology Co., Ltd.). Band intensities were semi-quantified using ImageJ software (version 1.53, National Institutes of Health). All western blot analyses were performed using the same batch of protein lysates. Within each figure panel, all target proteins and their corresponding loading controls were obtained from the same experimental run under identical conditions.

Rhodamine-phalloidin staining. Cellular surface area was assessed using rhodamine-phalloidin staining. Briefly, AC16 cardiomyocytes were washed twice with PBS and fixed with 4% paraformaldehyde for 20 min at room temperature. After three PBS washes, cells were permeabilized with 0.1% Triton X-100 in PBS for 15 min at room temperature. Following additional PBS washes, cells were incubated with rhodamine-phalloidin working solution (diluted 1:100 in PBS containing 1% BSA and 0.1% Triton X-100; cat. no. GC305010; Wuhan Servicebio Technology Co., Ltd.) for 60 min at room temperature. Nuclei were counterstained with DAPI for 5 min at 37˚C. Fluorescent images were captured using an Olympus fluorescence microscope (Olympus Corporation). Finally, cell surface areas were quantified using ImageJ software (version 1.53; National Institutes of Health).

WGA staining. Cells were cultured on slides under standard conditions (ISO 10 μM; 24 h; si-ABCC9 50 nmol/l; 24 h; 740Y-P 10 μM; 24 h; 37˚C) using the same culture medium as described for the other experiments. Once the cells reached the appropriate density, the medium was discarded, the culture medium was discarded and cells were washed twice with 1X PBS preheated to 37˚C. Subsequently, an appropriate amount of 4% paraformaldehyde was added to fix the slides at room temperature for 15 min. The cells were then washed three times with PBS to remove residual fixative. After the coverslips were dried, the central area was circled with a brush and a WGA staining solution diluted with PBS (G1730-100UL; Wuhan Servicebio Technology Co., Ltd.) was added. The solution was incubated at 37˚C in the dark for 30 min to label the cell membranes. After incubation, the cells were thoroughly washed three times with PBS to remove any unbound WGA. Subsequently, an anti-fluorescence quenching mounting medium containing DAPI (cat. no. P0131; Beyotime Biotechnology) was added, the sample was covered with a coverslip and images were observed under a laser confocal microscope (LSM 800; Zeiss AG). Finally, the ImageJ

software (version 1.53; National Institutes of Health) was used to perform quantitative analysis of the cell surface area.

MMP assessment. MMPs were assessed using an enhanced matrix metalloproteinase detection kit containing JC-1 (cat. no. C2006; Beyotime Biotechnology). After removing the culture medium, cells (30,000 cells per well) seeded in a 6-well plate were supplemented with 1 ml DMEM (Shanghai Basal Media Technologies Co., Ltd.) and 1 ml JC-1 staining solution. The cells were then incubated at 37˚C for 20 min. After removing the staining solution, the cells were washed twice with JC-1 staining buffer and observed under a fluorescence microscope (Olympus Corporation). Fluorescence intensity analysis was performed using ImageJ software (version 1.53, National Institutes of Health).

Flow cytometry of apoptosis. Cell apoptosis was assessed using an Annexin V-FITC/PI Apoptosis Detection Kit (cat. no. 40302; Shanghai Yeasen Biotechnology Co., Ltd.). AC16 cells in logarithmic growth phase were seeded into 6-well plates at a density of $3.5x10^5$ cells per well and cultured overnight at 37˚C. Following experimental treatments, cells were treated differently according to the experimental groups (ISO, 10 μM; 24 h; si-ABCC9 50 nmol/l; 24 h; 740Y-P 10 μM; 24 h; 37˚C). AC16 cells were digested using EDTA-free trypsin at 37˚C for 1 min, collected, and centrifuged at 300 x g for 5 min at 4˚C to remove the supernatant. The cells were then resuspended twice with PBS. In addition, the cells were incubated with 100 μl binding buffer (cat. no. 40302; Shanghai Yeasen Biotechnology Co., Ltd.) and 5 μl Annexin V/FITC for 10 min at room temperature in the dark. Then, 400 μl binding buffer and 5 μl PI were added and mixed for 5 min in the dark. This was followed and immediately analyzed using a BD LSRFortessa™ Fusion flow cytometer (BD Biosciences). Apoptosis rate was analyzed using FlowJo software (version 10.8.1; BD Biosciences). Cells were divided into four sections: Q1 (necrotic cells), Q2 (late apoptosis cells), Q3 (early apoptosis cells) and Q4 (live cells). The apoptosis rate=early apoptosis rate + late apoptosis rate.

Reactive oxygen species (ROS) level assessment. Intracellular ROS levels were measured using DCFH-DA. AC16 cells were plated in 12-well plates at $1.5x10^5$ cells per well and treated as described (ISO 10 μM, 24 h; si-ABCC9 50 nmol/l, 24 h; 740Y-P 10 μM, 24 h; 37˚C). After removing the culture medium, cells were incubated with 500 μl DCFH-DA (1:1,000 dilution in PBS) for 20 min at 37˚C in the dark. After washing three times with PBS, the cells were observed under an inverted fluorescence microscope (Olympus Corporation). Fluorescence intensity was analyzed using ImageJ software (version 1.53, National Institutes of Health).

Statistical analysis. All statistical analyses were performed using GraphPad Prism (version 9.1.1; Dotmatics). Data are expressed as the mean ± standard deviation of three independent replications of the experiment. Comparisons between groups were made using two-tailed unpaired Student's t-tests and one-way ANOVA, followed by Tukey's post hoc test. $P<0.05$ was considered to indicate a statistically significant difference.

Results

ABCC9 expression is elevated in the MH model. To investigate the expression of ABCC9 in MH, an *in vitro* model of ISO-induced cardiomyocyte hypertrophy was established. AC16 cardiomyocytes were treated with different concentrations of ISO (0, 5, 10, 20 and 40 μmol/l), and the inhibitory effect of ISO treatment on AC16 cells was observed in a concentration-dependent manner. After 24 h treatment with 10 μM ISO, no significant cytotoxicity was observed in AC16 cells, and cell viability showed no significant reduction compared with the control group (Fig. 1A). Based on previous studies (32,33) and the present preliminary experiment, a concentration of 10 μM ISO was considered non-toxic to cardiomyocytes, and therefore this concentration of ISO was selected to establish the MH model in subsequent experiments. To further investigate the effects of ISO-induced dynamic temporal changes on ABCC9 protein expression in AC16 cells, cardiomyocytes were treated with 10 μM ISO for different time periods (0, 12, 24 and 48 h). Western blot analysis revealed that ABCC9 expression began to significantly increase at 12 h, peaked at 24 h and remained at a significantly high level at 48 h (Fig. 1B and C). The 24-h treatment with 10 μM ISO appeared to be associated with significantly elevated ABCC9 expression, suggesting a potential role in the progression of ISO-induced cardiomyocyte hypertrophy. RT-qPCR was used to quantify the mRNA expression levels of cardiomyopathy markers ANP, BNP and β-MHC. The results showed that the mRNA expression levels of ANP, BNP and β-MHC in the ISO group were significantly higher compared with those in the control group (Fig. 1D). Changes in the surface area of AC16 cardiomyocytes were observed using confocal microscopy. AC16 cells were stained with rhodamine-phalloidin and WGA. Compared with the control group, the surface area of AC16 cells in the ISO group was significantly larger (Fig. 1E-H). Overall, the aforementioned findings indicated that the ISO-induced MH model had been successfully established and ABCC9 was significantly highly expressed in MH, suggesting that ABCC9 was closely related to the development of MH disease.

Effects of ABCC9 silencing on myocardial function and structure. Since ABCC9 was upregulated in AC16 hypertrophic cardiomyocytes, ABCC9 may regulate the progression of cardiomyocyte hypertrophy. To investigate the potential effects of ABCC9 on cardiac hypertrophy, ABCC9 loss-of-function was established using siRNA interference-mediated gene silencing. First, the knockdown rate of ABCC9-siRNA3 in cells treated with ISO was significant, compared with the non-significant reductions of ABCC9 expression mediated by ABCC9-siRNA1 and ABCC9-siRNA2, as observed by western blotting (Fig. 2A and B). Therefore, ABCC9-siRNA3 was selected for subsequent studies. Subsequently, western blotting results further validated the gene silencing efficiency of ABCC9-siRNA3 at up to 85% under control conditions (Fig. 2C and D), and ABCC9 knockdown significantly inhibited the overexpression of ABCC9 protein in AC16 cells induced by ISO (Fig. 2E and F). Notably, ABCC9 knockdown inhibited ISO-induced cardiomyocyte hypertrophic growth. The protein expression levels of ANP and BNP were significantly higher in the ISO and ISO + si-NC groups compared with the NC group, whereas ABCC9

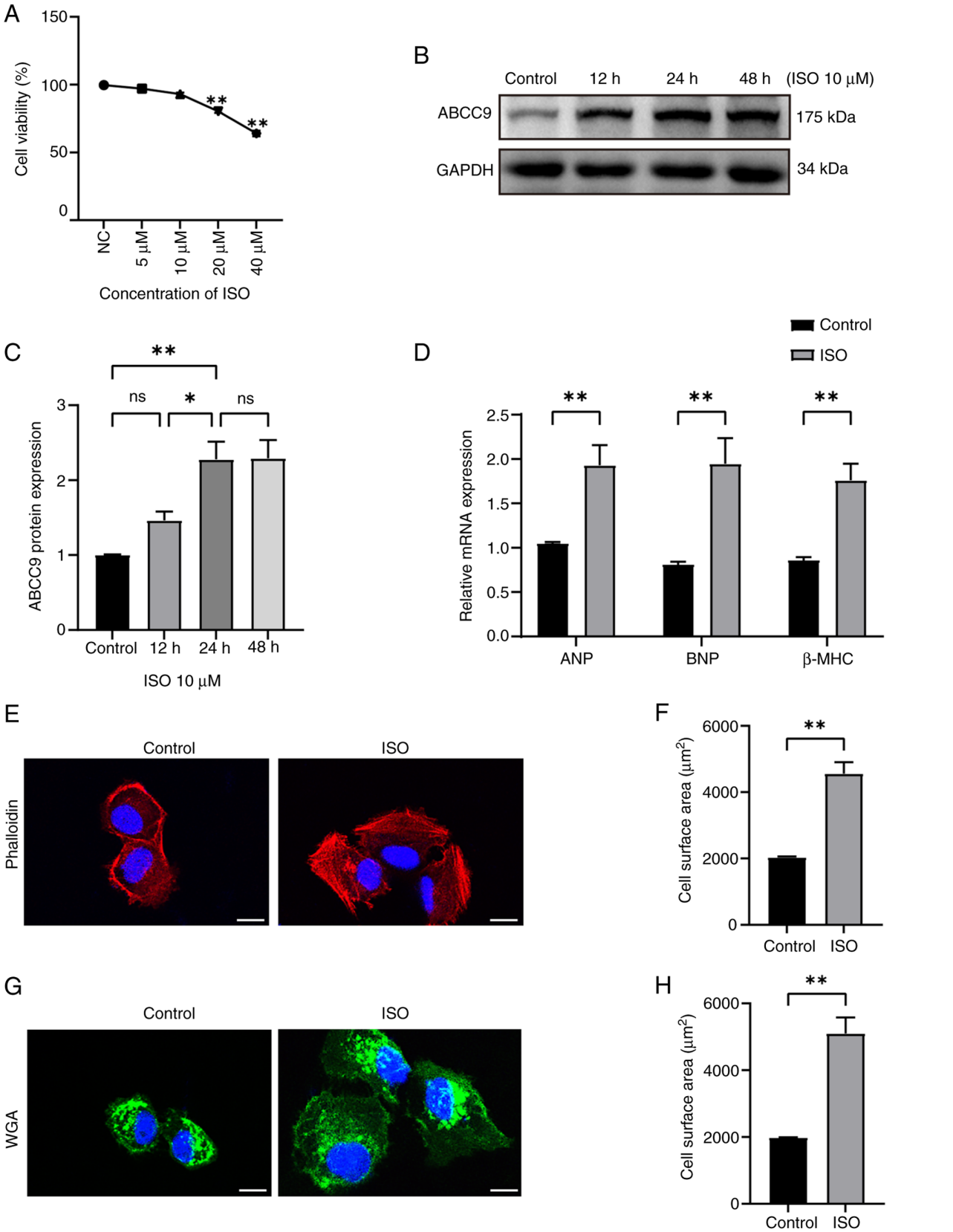

Figure 1. Elevated expression of ABCC9 in the ISO-induced myocardial hypertrophy model. (A) Cell Counting Kit-8 was used to determine the viability of ISO-induced AC16 cells. After treating AC16 cardiomyocytes with 10 μM ISO for different time periods, western blot analysis was performed to assess changes in ABCC9 protein expression. (B) Representative western blot image of ABCC9 and (C) semi-quantitative detection of ABCC9 protein expression levels using ImageJ software. (D) Evaluation of mRNA expression levels of ANP, BNP and β-MHC in ISO-treated AC16 cells using reverse transcription-quantitative PCR. After ISO stimulation, cardiomyocytes were stained with (E) rhodamine phalloidin and (F) cell surface area was analyzed. After ISO stimulation, cardiomyocytes were stained with (G) WGA and (H) cell surface area was analyzed. Fluorescent images of ISO-treated AC16 cells were obtained using a laser confocal microscope, and cell surface area was quantified using ImageJ software. Scale bar, 20 μm. AC16 cells were treated with ISO (10 μmol/l) for 24 h. n=3; *P<0.05 and **P<0.01 vs. control. ABCC9, ATP-binding cassette subfamily C member 9; NC, negative control; ns, not significant; ISO, isoproterenol; ANP, atrial natriuretic peptide; BNP, brain natriuretic peptide; β-MHC, β-myosin heavy chain; WGA, wheat germ agglutinin.

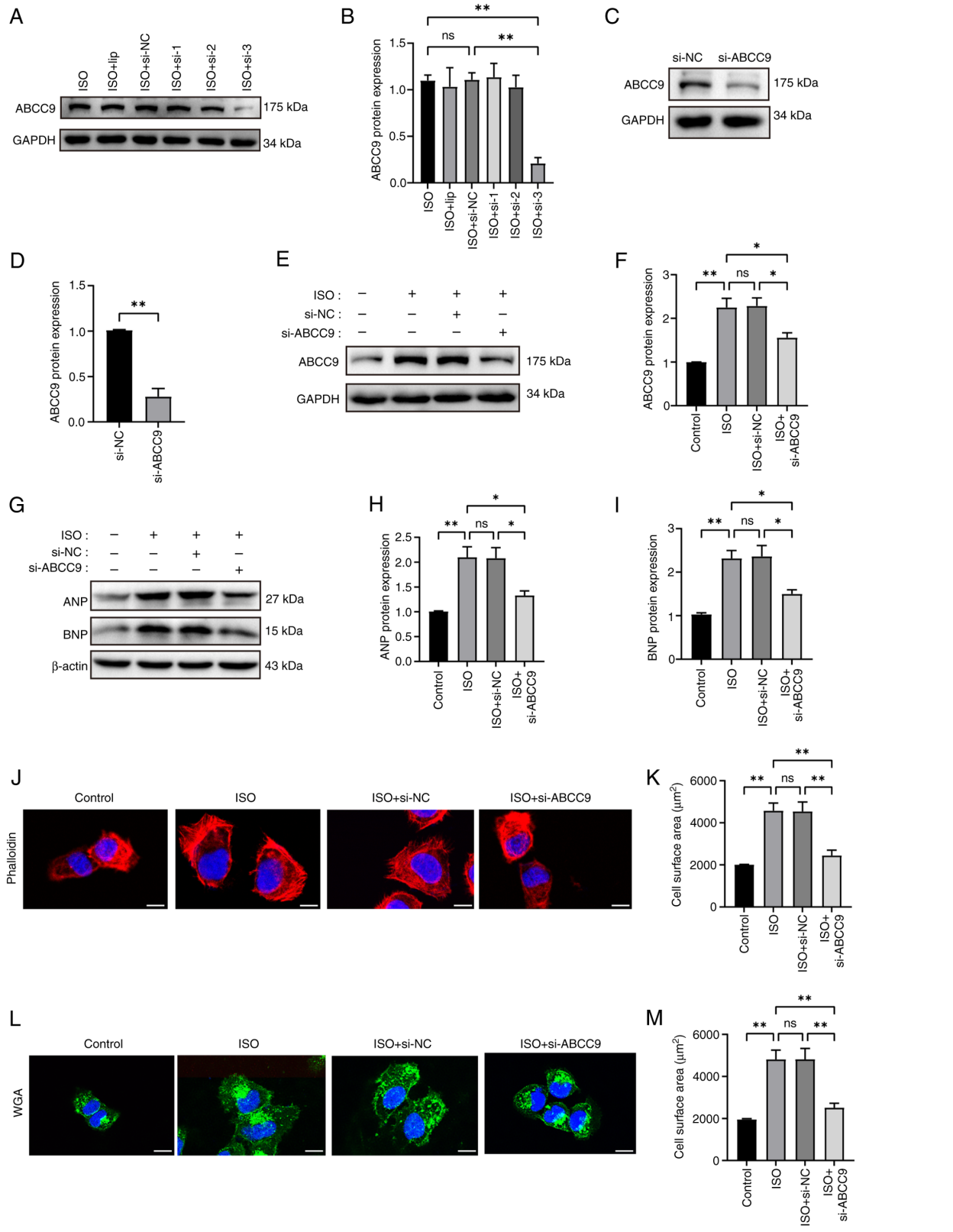

Figure 2. Silencing of ABCC9 attenuates ISO-induced myocardial hypertrophy in AC16 cells. (A) Western blot analysis assessed the transfection efficiency of ABCC9 knockdown. (B) ImageJ was used for semi-quantitative analysis of ABCC9 protein expression levels. (C) Western blotting and (D) semi-quantitative analysis confirmed the knockdown efficiency of ABCC9 si-3 transfection in normal cardiomyocytes. (E) Western blot analysis was used to assess the protein expression levels of ABCC9 in ISO-treated AC16 cells after ABCC9 knockdown. (F) ImageJ was used for semi-quantitative analysis of ABCC9 protein expression levels. (G) Representative western blot images of ANP and BNP. (H) ANP and (I) BNP protein expression levels were semi-quantified using ImageJ. Myocardial cells transfected with ABCC9-siRNA for 24 h were treated with (J) rhodamine-phalloidin and (K) analyzed quantitatively. Myocardial cells transfected with ABCC9-siRNA for 24 h were treated with (L) WGA staining and (M) analyzed quantitatively. The ISO-induced surface area of AC16 myocardial cells was detected using a laser confocal microscope. The cell surface area was quantified using ImageJ software. Scale bar, 20 μm. AC16 cells were treated with ISO (10 μmol/l) for 24 h. n=3; *P<0.05 and **P<0.01. NC, negative control; ns, not significant; ISO, isoproterenol; ABCC9, ATP-binding cassette subfamily C member 9; ANP, atrial natriuretic peptide; BNP, brain natriuretic peptide; si, small interfering RNA; WGA, wheat germ agglutinin; lip, Lipofectamine® 3000 transfection reagent.

knockdown significantly reduced the protein expression levels of ANP and BNP in AC16 cells (Fig. 2G-I). Rhodamine-phalloidin and WGA staining showed that the surface area of ISO-induced AC16 cells was significantly increased compared with the NC group, whereas the surface area of AC16 cardiomyocytes was significantly reduced after ABCC9 knockdown (Fig. 2J-M). Collectively, these findings suggest that silencing ABCC9 attenuated cardiomyocyte hypertrophy.

ABCC9 knockdown attenuates cardiomyocyte apoptosis, oxidative stress and mitochondrial dysfunction. The present study further investigated the role of silencing ABCC9 in ISO-induced AC16 cells using western blotting and quantified apoptosis-related proteins in different groups of AC16 cells. The results showed that, compared with the control group, the expression levels of Bax, caspase-3 and cleaved caspase-3 protein were significantly increased in ISO-induced AC16 cells, while the expression level of Bcl-2 was significantly decreased. Compared with the ISO group, the expression levels of Bax, caspase-3 and cleaved caspase-3 proteins were significantly reduced in the si-ABCC9 group, and Bcl-2 was significantly increased (Fig. 3A-E). To evaluate caspase-3 activation, the ratio of cleaved caspase-3/caspase-3 was analyzed. Notably, while both forms were elevated by ISO treatment, the cleaved caspase-3/caspase-3 ratio showed no significant difference (Fig. 3F), suggesting concurrent upregulation of caspase-3 protein alongside its activation. ABCC9 knockdown significantly reduced the levels of cleaved caspase-3, indicating suppression of the apoptotic signal. Flow cytometry analysis further supported the association between ABCC9 and apoptosis. The apoptosis rate, defined as the sum of early apoptotic (Annexin V^+/PI^-) and late apoptotic (Annexin V^+/PI^+) cells, was significantly higher in ISO-treated AC16 cells compared with in the control group. Specifically, early and late apoptotic cells accounted for 7.32 and 13.70%, respectively, compared with 1.54 and 3.28% in control cells. Knockout of ABCC9 significantly attenuated ISO-induced cardiomyocyte apoptosis, reducing the proportions of early and late apoptotic cells to 2.49 and 7.51%, respectively (Fig. 3G and H).

Furthermore, considering the role of oxidative stress in MH, the levels of ROS were measured in different groups of AC16 cells using DCFH-DA staining (Fig. 4A and B). The results of the present study showed that ISO stimulation significantly increased ROS production in AC16 cells. However, silencing of ABCC9 in AC16 cells reduced the stimulatory effect of ISO and significantly decreased ROS levels. To further investigate the effect of ABCC9 knockdown on mitochondrial function, JC-1 staining was used to assess MMP. Normal control cells exhibited red fluorescence, while cells with damaged mitochondrial membranes exhibited green fluorescence. Green fluorescence was clearly observed in cells from the ISO group, indicating a decrease in MMP, and the ISO-induced decrease in MMP was significantly alleviated by ABCC9 knockdown (Fig. 4C-E). These findings suggested that ABCC9 deficiency directly alleviated ISO-induced apoptosis and oxidative stress and improved mitochondrial function in cardiomyocytes *in vitro*.

ABCC9 knockdown attenuates MH by inhibiting the PI3K/AKT pathway. The PI3K/AKT pathway has been reported to serve a key role in the regulation of MH (34). To determine the potential mechanisms underlying the effects of ABCC9 on ISO-induced MH, the expression levels of PI3K/AKT signaling pathway proteins were examined. Protein phosphorylation of PI3K and AKT was significantly elevated in the ISO group compared with the control group. By contrast, ABCC9 knockdown significantly downregulated protein phosphorylation of PI3K and AKT, and neither ISO nor ABCC9 knockdown treatment affected the total level of PI3K or AKT, suggesting that PI3K/AKT signaling activity was affected by ABCC9 (Fig. 5A-C). In addition, to further elucidate whether the protective effect of silencing ABCC9 on cardiomyocytes was related to the inhibition of the PI3K/AKT signaling pathway, ISO-induced cardiomyocytes were treated with the PI3K/AKT pathway activator 740Y-P. Silencing of ABCC9-mediated reduction in PI3K/AKT expression was significantly reversed by 740Y-P (Fig. 5D-F). The present study found that p-PI3K/p-AKT protein expression was significantly elevated in the activator 740Y-P-treated group alone compared with the ISO + si-NC group. Thus, the protective effect of knocking down ABCC9 against ISO-induced MH was mediated by inhibiting the PI3K/AKT signaling pathway.

Notably, 740Y-P also blocked the effects of ABCC9 knockdown on hypertrophic gene expression and cardiomyocyte surface area size. The protein and mRNA expression levels of ANP, BNP and β-MHC were assessed using western blot analysis and RT-qPCR. The results showed that ABCC9 knockdown significantly reduced ISO-induced hypertrophic gene mRNA and protein expression compared with the si-NC group. Notably, co-treatment of the PI3K activator 740Y-P with si-ABCC9 significantly reversed the aforementioned inhibitory effects (Fig. 6A-F), and treatment with 740Y-P and ISO alone further aggravated the expression of hypertrophic markers. Rhodamine-phalloidin and WGA staining assays showed that the surface area of AC16 cardiomyocytes was significantly increased in the ISO + si-NC group compared with the NC group, but ABCC9 knockdown significantly reduced the ISO-induced increase in AC16 surface area. Similarly, co-treatment with 740Y-P significantly rescued the reduction in cell surface area caused by ABCC9 knockdown (Fig. 6G-J), whereas treatment with the activator 740Y-P and ISO alone significantly increased the cell surface area compared with the control group and thus exacerbated the MH. The present results suggested that ABCC9 knockdown attenuated ISO-induced MH by inhibiting PI3K/AKT signaling, whereas the PI3K activator 740Y-P partially reversed the protective effect. Overall, the aforementioned findings suggested that the protective effect of ABCC9 knockdown on MH was predominantly triggered by PI3K/AKT inhibition.

ABCC9 knockdown attenuates cardiomyocyte apoptosis and oxidative stress by inhibiting the PI3K/AKT signaling pathway and restoring MMP. To further investigate the protective effect of ABCC9 knockdown on ISO-stimulated AC16 cells, the present study tested whether activation of PI3K activity counteracted the amelioration of apoptosis and oxidative stress by ABCC9 knockdown. Western blotting results showed that ABCC9 knockdown significantly alleviated the apoptotic effects of ISO stimulation on AC16 cells, as evidenced by reduced expression levels of Bax, cleaved caspase-3 and caspase-3 protein, along with increased

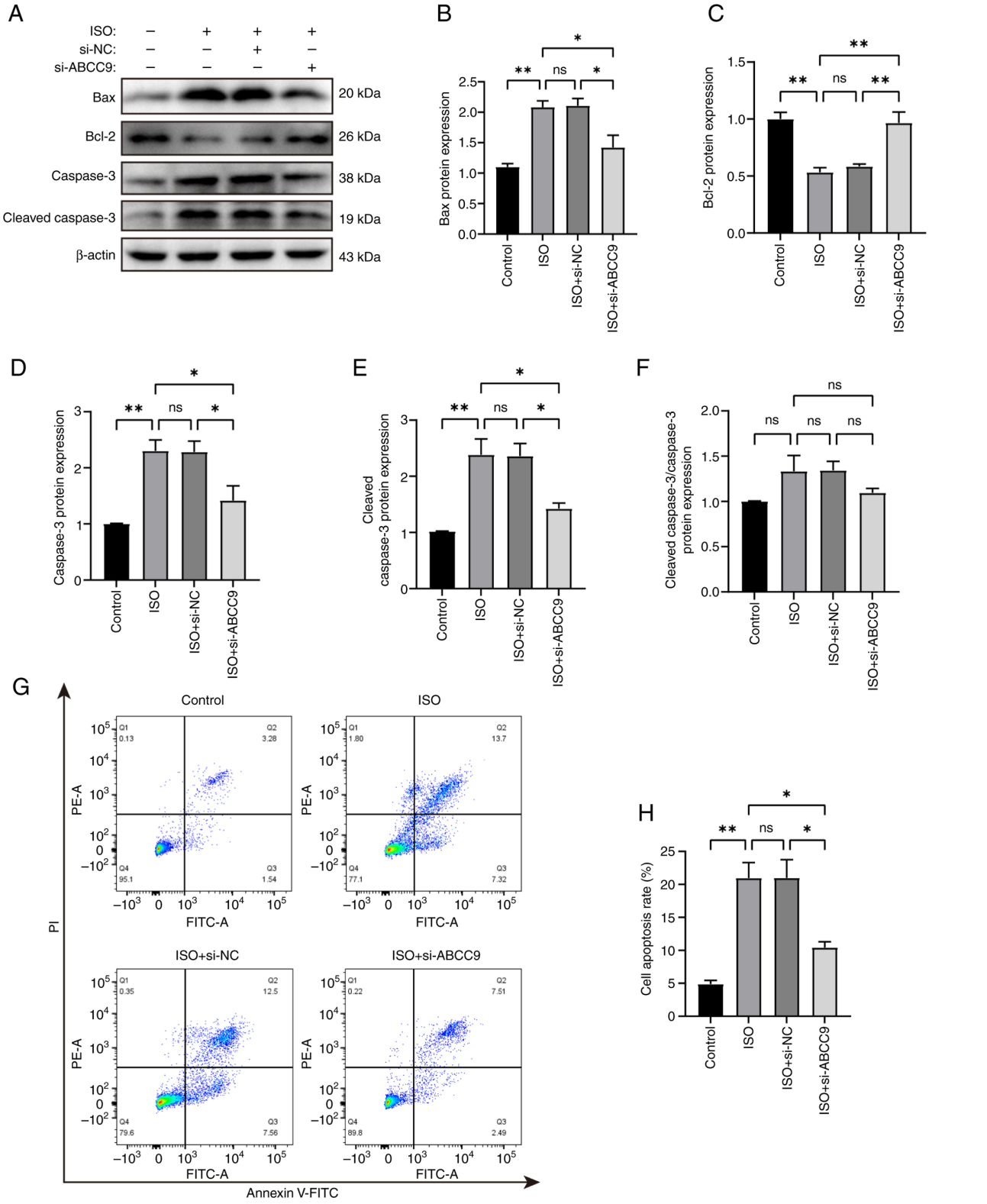

Figure 3. ABCC9 knockdown inhibits apoptosis in cardiomyocytes. (A) Western blot analysis was used to assess changes in the expression of apoptosis-related proteins Bax, Bcl-2, caspase-3 and cleaved caspase-3 in AC16 cells. ImageJ was used for semi-quantitative analysis of the expression levels of (B) Bax, (C) Bcl-2, (D) caspase-3, (E) cleaved caspase-3 proteins and (F) cleaved caspase-3/caspase-3 ratio. (G) Representative flow cytometry images and (H) quantitative analysis of Annexin V-FITC/PI staining in AC16 cells. AC16 cells were treated with ISO (10 μmol/l) for 24 h. n=3; *P<0.05 and **P<0.01. NC, negative control; ns, not significant; ISO, isoproterenol; ABCC9, ATP-binding cassette subfamily C member 9; Bax, Bcl-2 associated X protein; Bcl-2, B-cell lymphoma 2 protein; si, small interfering RNA.

expression levels of Bcl-2 protein compared with the ISO + si-NC group. Pretreatment with the activator 740Y-P significantly reversed this inhibitory effect. Notably, treatment with 740Y-P and ISO significantly increased the expression of these pro-apoptotic proteins and significantly reduced Bcl-2 expression, indicating that PI3K activation intensified ISO-induced

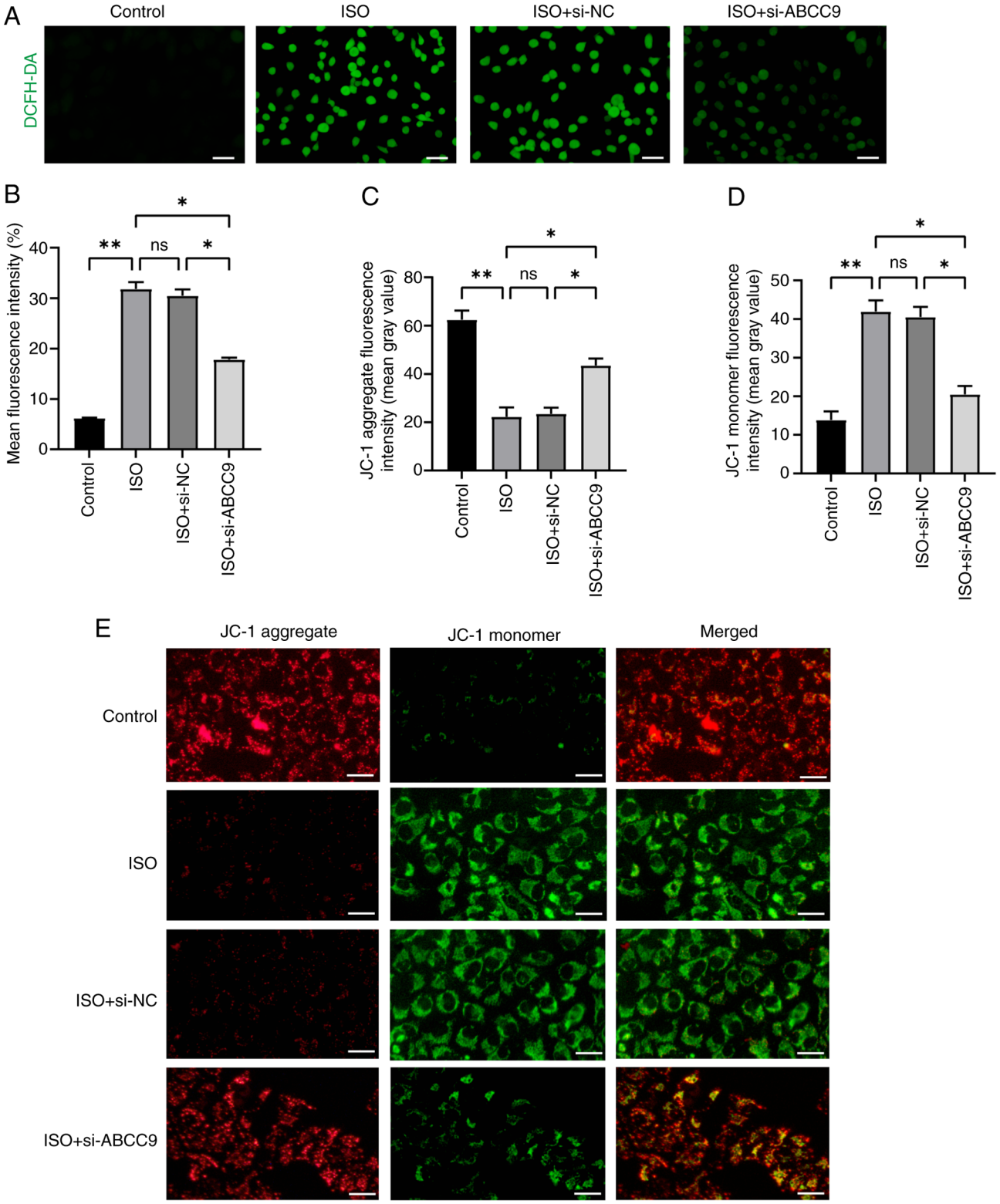

Figure 4. ABCC9 knockdown alleviates oxidative stress and mitochondrial damage in cardiomyocytes. (A) Representative fluorescent images of DCFH-DA staining and (B) semi-quantification of intracellular reactive oxidative species levels in AC16 cells. Fluorescence intensity analysis of (C) JC-1 aggregate and (D) JC-1 monomer on mitochondrial membrane potential. (E) Mitochondrial membrane potential representative fluorescence images. Scale bar, 100 μm. AC16 cells were treated with ISO (10 μmol/l) for 24 h. n=3; *P<0.05 and **P<0.01. NC, negative control; ns, not significant; ABCC9, ATP-binding cassette subfamily C member 9; ISO, isoproterenol; DCFH-DA, 2',7'-dichlorodihydrofluorescein diacetate; si, small interfering RNA.

injury (Fig. 7A-E). Consistent with the observations in Fig. 3, the ratio of cleaved caspase-3/caspase-3 also showed no significant difference among groups treated with ISO, si-ABCC9 and 740Y-P (Fig. 7F). In addition, changes in apoptotic cell quantity were assessed using flow cytometry. The results showed that the rate of ISO-induced apoptosis in AC16 cardiomyocytes was significantly increased, and silencing ABCC9 effectively inhibited ISO-induced apoptosis in AC16 cells.

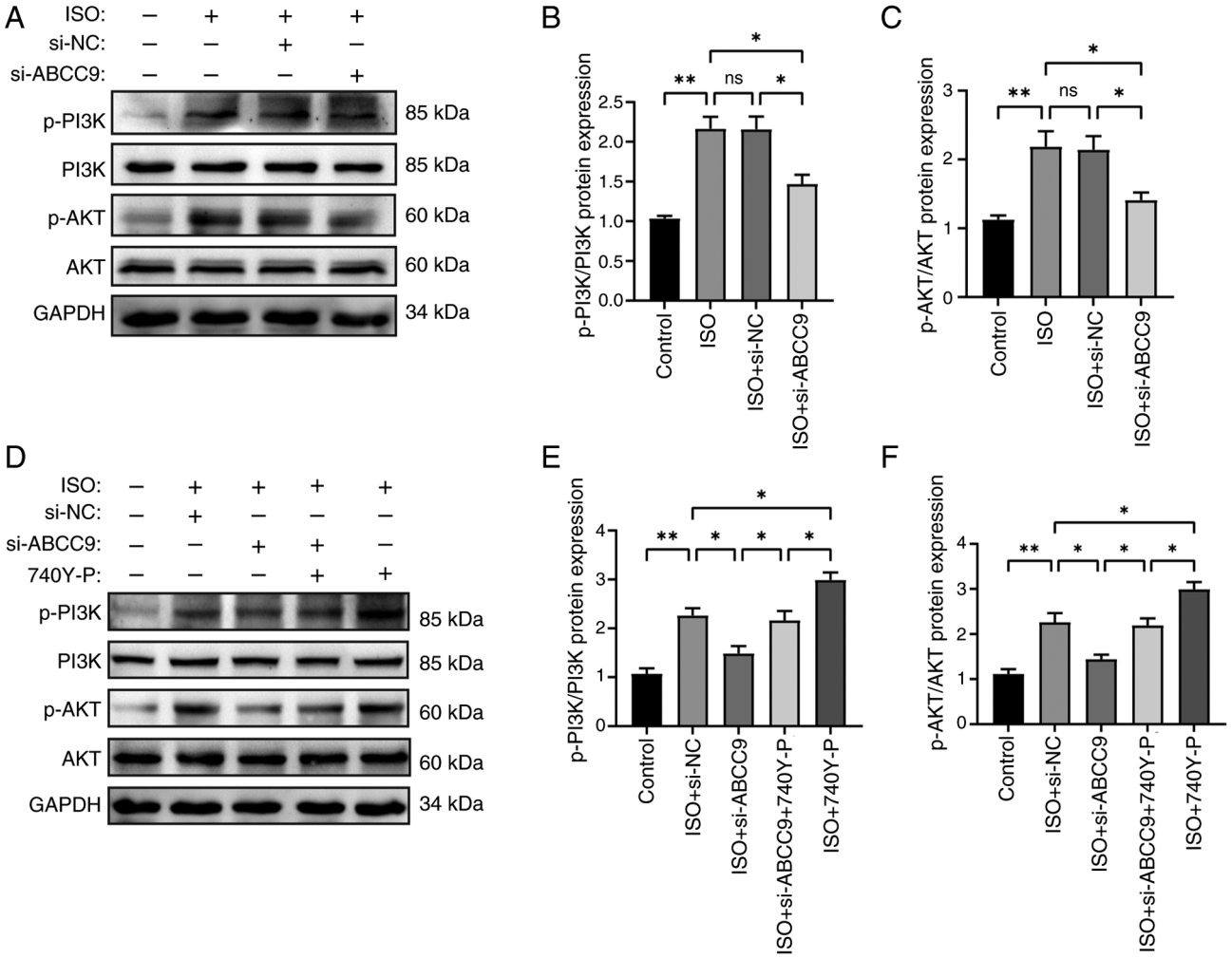

Figure 5. Effect of 740Y-P and ABCC9 knockdown on PI3K/AKT signaling pathway proteins. (A) Western blot bands of PI3K, p-PI3K, AKT and p-AKT in AC16 cells. Semi-quantitative analysis of (B) p-PI3K and (C) p-AKT protein expression using ImageJ. (D) Western blotting with 740Y-P showed a reversal of the protective effect of ABCC9 knockdown on ISO-induced AC16 cells. (E) Semi-quantitative analysis of p-PI3K and (F) p-AKT protein expression with 740Y-P treatment. AC16 cells were treated with ISO (10 μmol/l) for 24 h. n=3; *P<0.05 and **P<0.01. NC, negative control; ns, not significant; ABCC9, ATP-binding cassette subfamily C member 9; ISO, isoproterenol; si, small interfering RNA; PI3K, phosphatidylinositol-3-kinase; AKT, protein kinase B; p-, phosphorylated.

Compared with the si-ABCC9 group, cardiomyocyte apoptosis was significantly aggravated by pretreatment with the PI3K activator 740Y-P. Similarly, treatment with activator 740Y-P alone in ISO-treated cells further increased the number of apoptotic cells (Fig. 7G and H). These results indicate that the activation of PI3K activity by 740Y-P significantly reversed the therapeutic effect of knocking down ABCC9.

Meanwhile, ROS assay results showed that ABCC9 knockdown significantly reduced ROS levels in ISO-treated AC16 cells, but its effect was attenuated in the presence of 740Y-P (Fig. 8A and B). To further investigate the protective mechanism of ABCC9 knockdown against apoptosis, MMP was analyzed in cardiomyocytes treated with 740Y-P. Notably, compared with the ISO + si-ABCC9 group, pre-treatment with the PI3K activator 740Y-P significantly reversed the protective effect of ABCC9 knockdown on mitochondrial function (Fig. 8C-E). Furthermore, compared with the si-NC group, the use of activator 740Y-P and ISO also significantly exacerbated ROS production and mitochondrial dysfunction. The present results suggested that ABCC9 knockdown protected the myocardium by inhibiting the PI3K/AKT signaling pathway and alleviating mitochondrial dysfunction, while the PI3K activator 740Y-P partially reversed this effect. Overall, ABCC9 knockdown inhibited the PI3K/AKT signaling pathway, restored the MMP and thereby alleviated cardiomyocyte apoptosis and oxidative stress.

Discussion

The present study demonstrated that ABCC9 knockdown attenuated MH by reducing cardiomyocyte apoptosis and ROS production. This protective effect was mediated through inhibition of PI3K/AKT pathway phosphorylation and the subsequent improvement of mitochondrial function, thereby protecting cardiomyocytes from ISO-induced pathological changes. The framework of ABCC9-mediated regulation of the PI3K/AKT signaling pathway in ISO-induced MH is shown in Fig. 9.

MH, a well-established risk factor for CVD, is associated with markedly increased morbidity and mortality rates. However, the precise pathophysiological mechanisms of MH are yet to be fully elucidated. Although numerous

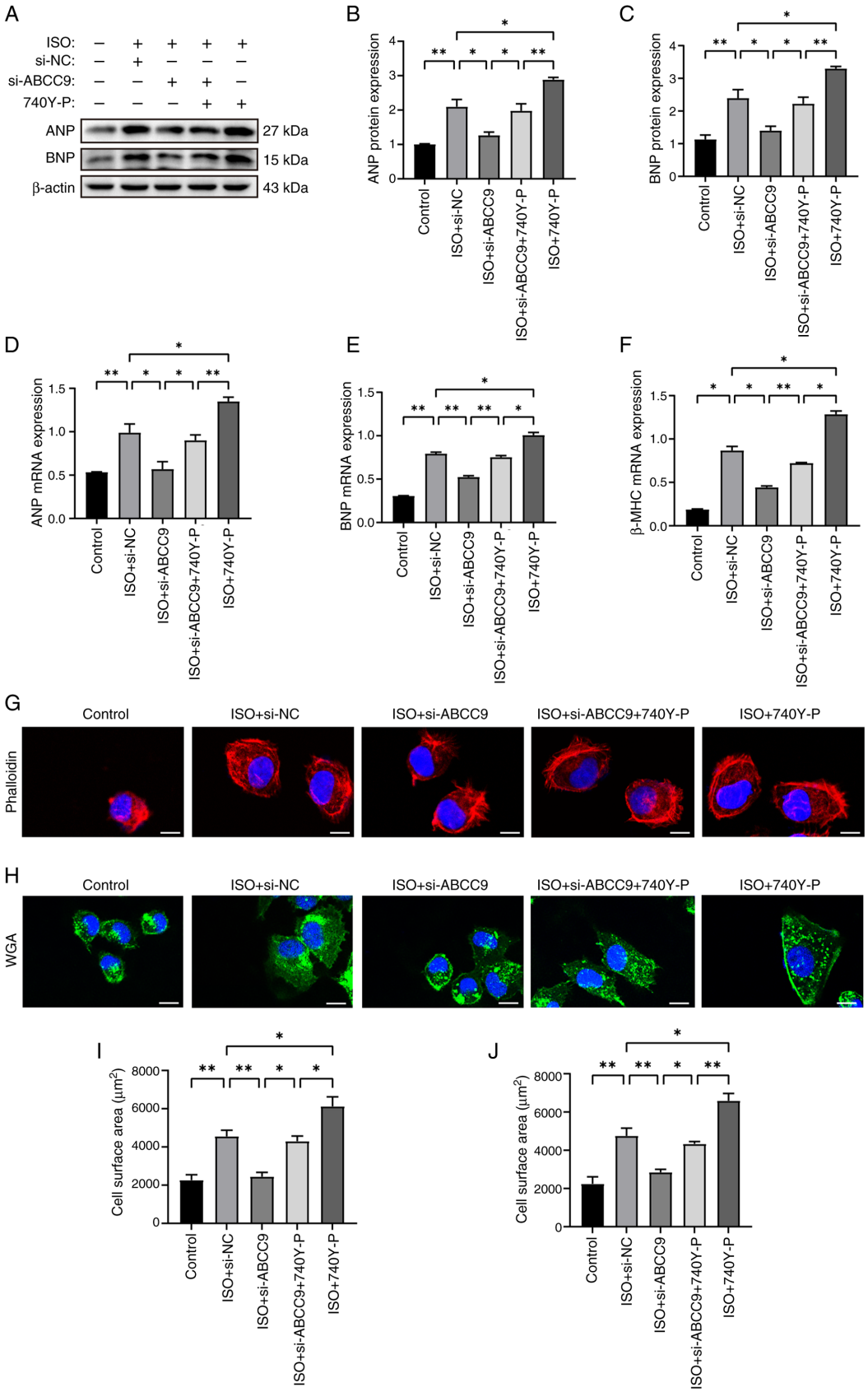

Figure 6. ABCC9 knockdown attenuates myocardial hypertrophy by inhibiting PI3K/AKT signaling pathway. (A) Western blot bands showing the effect of 740Y-P on ANP and BNP protein expression. (B) Semi-quantitative analysis of ANP and (C) BNP protein expression. Reverse transcription-quantitative PCR was used to assess the mRNA levels of the hypertrophic genes (D) ANP, (E) BNP and (F) β-MHC in 740Y-P treated AC16 cells. After transfection and 740Y-P pretreatment, AC16 cells were stained with (G) rhodamine phalloidin and (H) WGA, and fluorescence images of si-ABCC9 and 740Y-P-treated AC16 cells were obtained using a laser confocal microscope. Quantitative analysis of cell surface area in (I) rhodamine phalloidin and (J) WGA stained samples using ImageJ software. Scale bar, 20 μm. AC16 cells were treated with ISO (10 μmol/l) for 24 h. n=3; *P<0.05 and **P<0.01. NC, negative control; ABCC9, ATP-binding cassette subfamily C member 9; ISO, isoproterenol; ANP, atrial natriuretic peptide; BNP, brain natriuretic peptide; β-MHC, β-myosin heavy chain. si, small interfering RNA; WGA, wheat germ agglutinin.

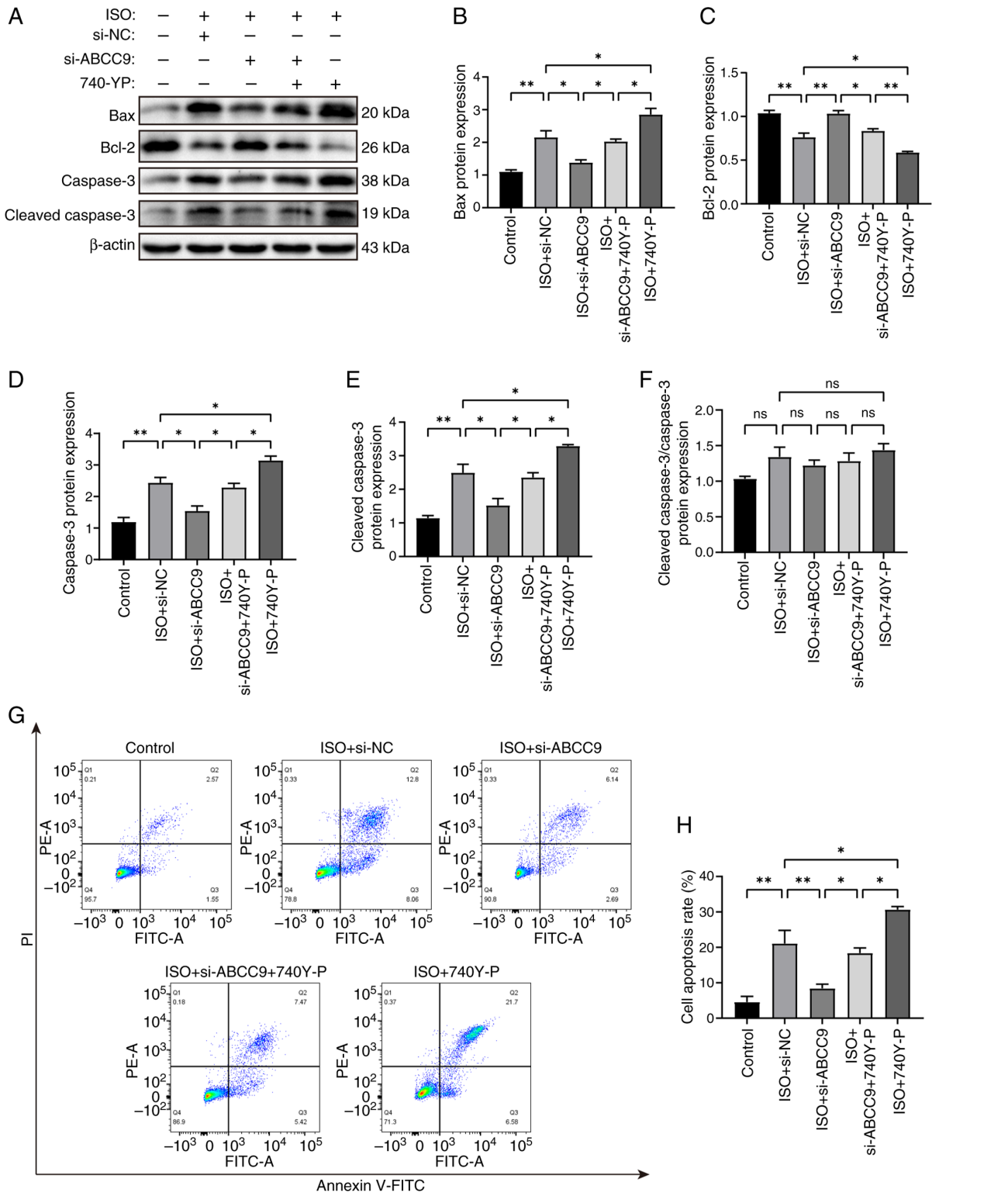

Figure 7. ABCC9 knockdown attenuates apoptosis in cardiomyocytes by inhibiting the PI3K/AKT pathway and alleviating mitochondrial dysfunction. (A) Western blot bands showing the effect of 740Y-P on the expression of the apoptosis-related proteins Bax, Bcl-2, caspase-3 and cleaved caspase-3 in AC16 cells. Semi-quantitative analysis of (B) Bax, (C) Bcl-2, (D) caspase-3, (E) cleaved caspase-3 proteins expression levels and (F) cleaved caspase-3/caspase-3 ratio was performed using ImageJ. (G) Representative flow cytometry images of Annexin V/PI staining and (H) quantification of apoptosis rate in AC16 cells. AC16 cells were treated with ISO (10 μmol/l) for 24 h. n=3; *P<0.05 and **P<0.01. NC, negative control; ns, not significant; ISO, isoproterenol; ABCC9, ATP-binding cassette subfamily C member 9; Bax, Bcl-2 associated X protein; Bcl-2, B-cell lymphoma 2 protein; DCFH-DA, 2',7'-dichlorodihydrofluorescein diacetate; si, small interfering RNA.

pharmacological interventions for MH exist, including angiotensin-converting enzyme inhibitors, β-adrenergic receptor (β-AR) blockers, calcium channel blockers and histone deacetylase inhibitors (35-37), these therapies present several clinical limitations and an effective treatment strategy for MH remains elusive.

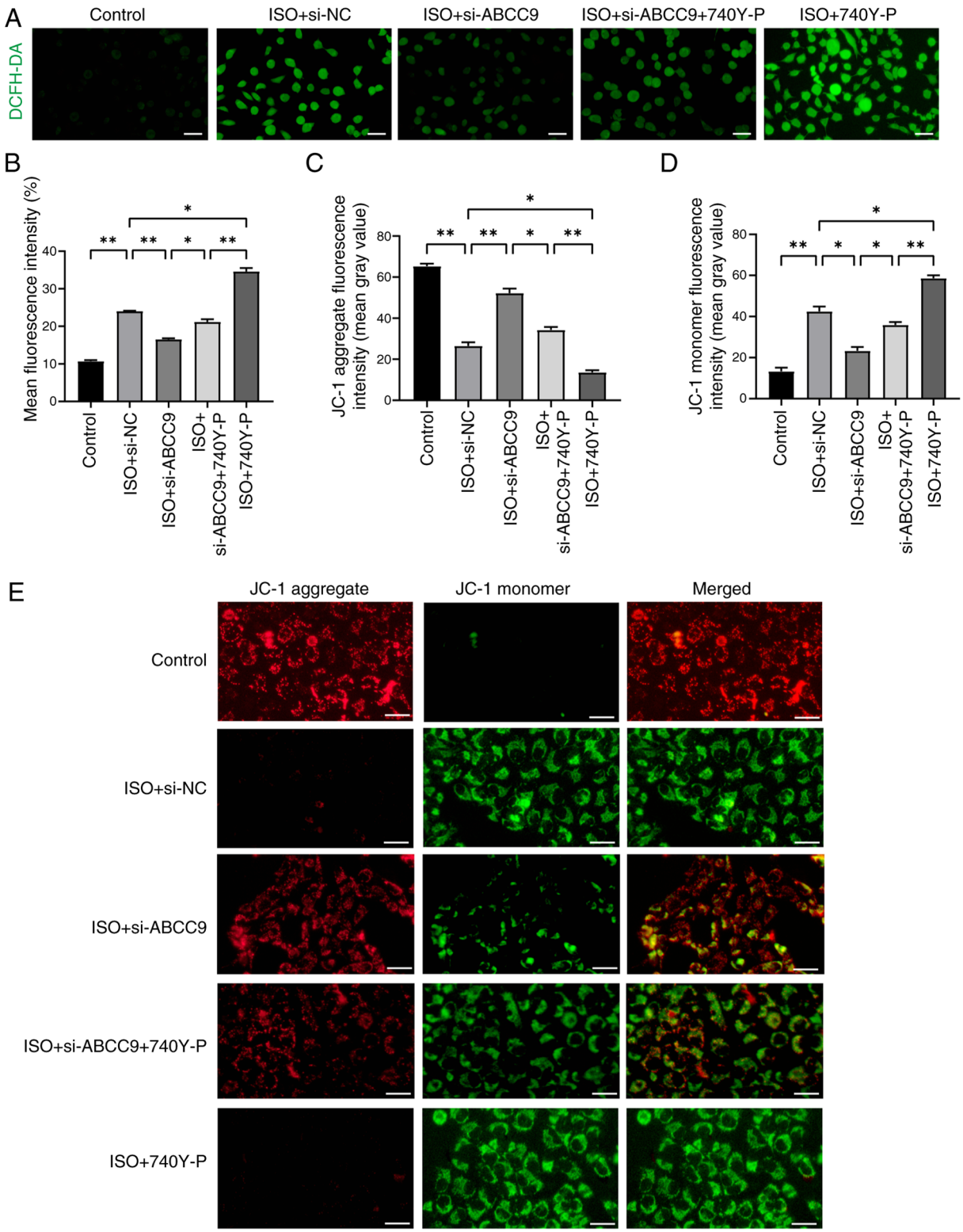

Figure 8. ABCC9 knockdown attenuates oxidative stress in cardiomyocytes by inhibiting the PI3K/AKT pathway and alleviating mitochondrial dysfunction. (A) Representative images of staining for reactive oxygen species and (B) fluorescence intensity analysis. After treatment with 740Y-P, the fluorescence intensity of (C) JC-1 aggregate and (D) JC-1 monomer of mitochondrial membrane potential in cardiomyocytes was analyzed. (E) Mitochondrial membrane potential representative fluorescence images. Scale bar, 100 μm. AC16 cells were treated with ISO (10 μmol/l) for 24 h. n=3; *P<0.05 and **P<0.01. NC, negative control; ISO, isoproterenol; ABCC9, ATP-binding cassette subfamily C member 9; DCFH-DA, 2',7'-dichlorodihydrofluorescein diacetate; si, small interfering RNA.

β-ARs, members of the G protein-coupled receptor family, serve as the primary cardiac receptors (38). The β-AR signaling pathway serves an important role in cardiac remodeling progression, with excessive activation leading to pathological cardiac hypertrophy and fibrosis (39), ultimately resulting in HF. While β-AR agonists are non-selective activators of these

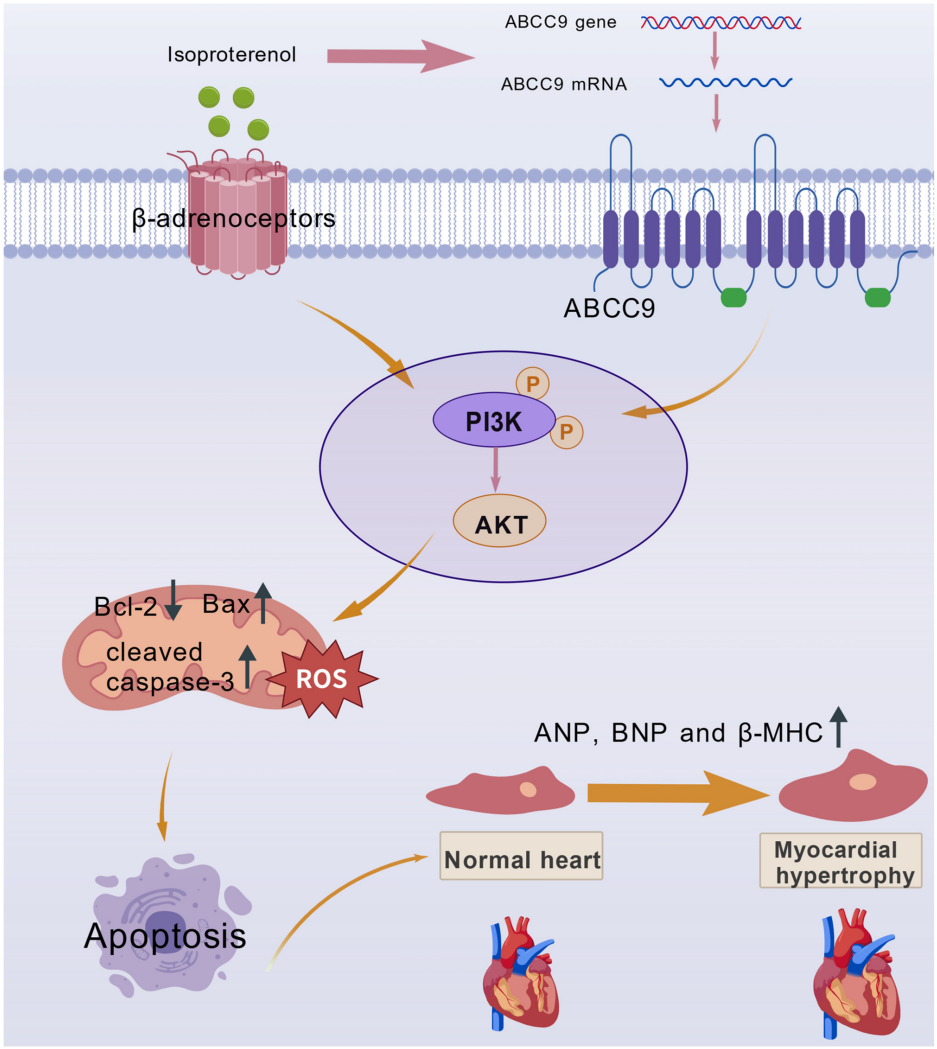

Figure 9. Schematic diagram describing the PI3K/AKT signaling pathway mechanism by which ABCC9 acts on MH. ISO binds to the cellular β-adrenergic surface receptor of cardiomyocytes, while ABCC9 is highly expressed in ISO-mediated cardiomyocytes, which triggers apoptosis and oxidative stress through activation of the PI3K/AKT pathway and results in mitochondrial dysfunction, ultimately leading to MH. ISO, isoproterenol; ABCC9, ATP-binding cassette subfamily C member 9; ANP, atrial natriuretic peptide; BNP, brain natriuretic peptide; β-MHC, β-myosin heavy chain; Bax, Bcl-2 associated X protein; Bcl-2, B-cell lymphoma 2 protein; ROS, reactive oxygen species; P, phosphate group; MH, myocardial hypertrophy.

receptors (40) that primarily function through sympathetic nervous system (SNS) activation, chronic SNS stimulation contributes to progressive cardiac dysfunction and structural deterioration, further exacerbating MH (41). It has been demonstrated that ISO is widely used to induce MH (42-44). In the present study, 10 μM ISO was selected for AC16 cell treatment to establish the MH model based on the results of the CCK-8 assay. ISO-induced MH is characterized by markedly elevated ROS levels in cardiomyocytes (45), increased apoptotic activity (46) and upregulated pro-inflammatory cytokine expression (47). Without intervention, severe prolonged MH progresses to cardiac dysfunction, myocardial infarction and HF (48), underscoring the notable need for developing effective therapeutic strategies for MH patients.

As a member of the ABC family of transporter proteins, ABCC9 mediates specific cardiovascular phenotypes characterized by left ventricular dilatation, increased ventricular mass and enhanced cardiac contractility (49).The ABCC9 gene has been implicated in various cardiac pathologies (27,28), and the present investigation revealed a strong association between ABCC9 expression levels and drug-induced MH, with expression positively associated with both MH severity and duration. Under pathological conditions such as myocardial infarction and HF, cardiomyocytes exhibit hypertrophic responses with a marked increase in the mRNA and protein expression of atrial ANP, β-MHC and ventricular BNP (50), biomarkers that maintain stable expression levels in normal cardiomyocytes (51). The results of the present study demonstrated that ISO treatment induced hypertrophic responses characterized by elevated ANP and BNP expression. Previous studies have established that MH progression is initially marked by increased cardiomyocyte surface area (52), a morphological change that directly reflects hypertrophic development. Notably, the present study provided, to the best of our knowledge, the first demonstration that ABCC9 siRNA transfection in cardiomyocytes significantly attenuated the expression of the hypertrophic markers ANP, BNP and β-MHC. Furthermore, ABCC9 knockdown effectively suppressed hypertrophic cardiomyocyte enlargement, demonstrating protective effects against ISO-induced MH.

The pathological mechanisms underlying MH primarily involve cardiomyocyte apoptosis, ROS generation and mitochondrial dysfunction (53). Due to its exceptionally high metabolic demands, cardiac tissue generates substantial ROS levels and remains particularly vulnerable to oxidative damage (54). Under pathological conditions, excessive ROS accumulation overwhelms cellular antioxidant defenses, resulting in oxidative stress and mitochondrial impairment (55), thereby accelerating hypertrophic progression. In the present study, oxidative stress was observed in ISO-treated AC16 cells, whereas ABCC9 knockdown effectively attenuated the ISO-induced increase in ROS levels and the proportion of ROS-positive cells.

Persistent oxidative stress compromises mitochondrial integrity, inhibits ATP synthesis and triggers apoptotic pathways, collectively worsening cardiac dysfunction (56). Cardiomyocyte apoptosis represents a well-established contributor to HF pathogenesis, with apoptotic acceleration in hypertrophic cardiomyopathy ultimately precipitating systolic impairment (57). This programmed cell death process is regulated through multiple mechanisms, including mitochondrial dysfunction, caspase activation and modulation of the apoptosis-related factors Bcl-2, Bax, caspase-3 and cleaved caspase-3 (58). The findings of the present study demonstrated that ABCC9 knockdown significantly reduced ISO-induced apoptosis, as shown by decreased Bax, caspase-3 and cleaved caspase-3 expression and increased Bcl-2 levels, and supported through Annexin V/PI staining with flow cytometric analysis. Furthermore, MMP measurements indicated that ABCC9 knockdown alleviated ISO-induced mitochondrial damage in cardiomyocytes. Notably, the ISO + si-NC group exhibited no cytotoxic effects at standard doses compared with ISO-treated cells. The simultaneous elevation of caspase-3 and cleaved caspase-3 expression levels may have reflected a dynamic equilibrium in ISO-induced MH. Under stress conditions, cardiomyocytes may have upregulated caspase-3 transcription via pathways such as the NF-κB or p53 pathways, while a portion of caspase-3 was cleaved during apoptosis. This mechanism would have resulted in sustained caspase-3 synthesis alongside partial activation, reflecting the coexistence of hypertrophy and apoptosis during the pathological process. These results positioned ABCC9 as a promising therapeutic target with a favorable safety profile for mitigating ISO-induced cardiomyocyte injury and suppressing hypertrophic progression.

The signaling mechanisms underlying MH are highly complex. Substantial evidence implicates the PI3K/AKT pathway as a central regulator of cardiac remodeling through its influence on MH progression, fibrotic changes, oxidative stress and inflammatory responses (59). PI3K, in particular, has been shown to contribute notably to oxidative stress while also driving the development of cardiac hypertrophy and HF (60). As an important downstream effector of PI3K, AKT further participates in hypertrophic processes by modulating diverse cellular metabolism, proliferation, survival, growth and angiogenesis (61). Furthermore, activation of the PI3K/AKT axis by various extracellular ligands such as lipopolysaccharide or CpG oligodeoxynucleotides enhances dendritic cell activity, which in turn amplifies immune and inflammatory reactions (62). Based on these findings, the present study hypothesized that ABCC9 knockdown might exert cardioprotective effects through modulation of p-PI3K/p-AKT levels. By examining the levels of p-PI3K and p-AKT proteins in AC16 cardiomyocytes, the present study found that the PI3K/AKT signaling pathway was activated in ISO-induced MH and that ABCC9 knockdown attenuated this effect. These experimental results supported the hypothesis that ABCC9 regulated MH through PI3K/AKT signaling pathway modulation.

It is notable that ABCC9 knockdown alleviated MH by inhibiting the PI3K/AKT signaling pathway, an effect likely mediated through the regulation of key AKT downstream effector molecules. Glycogen synthase kinase-3β (GSK-3β), a negative regulator of cardiac hypertrophy, is a downstream target of AKT; its activity is suppressed by AKT-mediated phosphorylation (63). Active GSK-3β has been demonstrated to directly inhibit pathological MH by preventing the nuclear translocation of pro-hypertrophic transcription factors, such as nuclear factor of activated T-cells (64). Furthermore, AKT phosphorylates the FoxO1 transcription factor (65), an important regulator of autophagy, metabolism and cell survival. Consequently, FoxO1 serves an important role in modulating MH and fibrosis in mice via the PI3K/AKT pathway (66). These processes collectively constitute an important defense mechanism against MH.

The mammalian target of rapamycin complex 1 (mTORC1), a notable downstream target of AKT, serves as a central regulator of protein synthesis and cell growth (67). Pharmacological inhibition of the mTORC1 signaling pathway has been shown to ameliorate pathological MH (68). The observed inhibition of AKT in the present study suggested a concomitant reduction in mTORC1 signaling activity, which would directly suppress the hypertrophic translational machinery. Additionally, AKT can activate NF-κB through the IKK pathway (69). As a classic pro-inflammatory and pro-survival transcription factor, NF-κB contributes to myocardial dysfunction in advanced HF (70). Thus, the AKT inhibition resulting from ABCC9 knockdown may have attenuated NF-κB signaling, thereby mitigating inflammatory responses and functional impairment in the hearts of hypertrophic mice. In summary, the inhibition of the PI3K/AKT pathway following ABCC9 knockdown is proposed to mitigate MH by coordinately regulating key nodal points downstream of AKT, including GSK-3β, FoxO1, mTOR and NF-κB. Consequently, future studies directly assessing the phosphorylation status and activity of these effector proteins are warranted to precisely elucidate the molecular mechanisms downstream of ABCC9.

It has been demonstrated that cell survival depends predominantly on the Bcl-2 family of apoptosis regulators (71) and that Bcl-2 is involved in cardiac hypertrophy as a key downstream effector of the PI3K/AKT signaling pathway (72). Subsequently, the present study further investigated whether ABCC9 knockdown could mitigate cardiomyocyte apoptosis and oxidative damage by improving mitochondrial injury through modulation of the PI3K/AKT pathway. Consistently, the present study showed that ABCC9 knockdown downregulated PI3K/AKT pathway protein expression while attenuating ISO-induced mitochondrial dysfunction, oxidative stress and apoptosis, supporting its potential to alleviate ISO-induced MH by enhancing the anti-apoptotic and antioxidant systems.

Although AKT has been shown to exert cardioprotective effects by promoting physiological hypertrophy and survival signaling, the outcomes of AKT signaling depend on the duration, frequency and intensity of AKT pathway activation. For example, short-term AKT activation promotes adaptive hypertrophy, whereas long-term AKT activation or high-levels of expression have been associated with pathological hypertrophy and HF (73-75). In the present study, this hypothesis was driven by the observation that reactivation of PI3K/AKT signaling with 740Y-P partially reversed the protective effects of ABCC9 knockdown-restoring ISO-induced ROS accumulation, mitochondrial dysfunction, and apoptosis. These results suggest that while short-term AKT activation may promote cell survival, prolonged excessive activation may lead to myocardial cell apoptosis, potentially mediated through mitochondrial dysfunction and increased oxidative stress. Supporting this view, studies have shown that high levels of ROS can promote the reversal of MMP by activating MAPK, resulting in cytochrome *c* release and the activation of caspase-3, which in turn trigger apoptosis (76,77). Under sustained pathological stress, chronic and excessive AKT signaling may become maladaptive, leading to metabolic dysfunction, increased oxidative stress and ultimately mitochondrial dysfunction (78,79), thereby triggering cardiomyocyte apoptosis.

To further verify whether activation of the PI3K/AKT signaling pathway eliminated the protective effect of ABCC9 knockdown, the PI3K/AKT pathway was activated using the specific agonist 740Y-P. 740Y-P is a PI3K/AKT pathway activator that has been reported to activate the enzyme *in vitro* by binding to the Src homology 2 structural domain of the p85 regulatory subunit of PI3K (80), thereby initiating the PI3K/AKT signaling pathway. In the present study, oxidative stress and MMP were partially restored and apoptosis was reduced in cells treated by transfection with ABCC9 siRNA. Notably, 740Y-P not only counteracted ABCC9 knockdown-mediated suppression of p-PI3K and its downstream target p-AKT but also reversed the protective effects of ABCC9 knockdown on apoptosis, oxidative stress and MMP. These results provided notable evidence that ABCC9 knockdown alleviated ISO-induced MH partly by modulating the PI3K/AKT pathway, which subsequently improved mitochondrial function, thereby reducing apoptosis and oxidative stress.

Although the data of the present study showed that knockdown of the ABCC9 gene attenuated MH by inhibiting the PI3K/AKT signaling pathway, thereby regulating apoptosis, MMP and oxidative stress, the role of the classic function of ABCC9, as a regulatory subunit of KATP channels, has not yet been directly assessed in this process. The SUR2 protein encoded by ABCC9 forms the KATP channel in conjunction with the Kir6.2 subunit, which serves a central role in linking cellular metabolic state to membrane potential, thereby regulating processes such as calcium influx, vascular tone (81), insulin secretion and cellular protection (82). The phenotype observed in the present study could theoretically have also arisen from cellular electrophysiological changes caused by altered KATP channel activity (83), so the contribution of ion channel activity cannot be entirely ruled out. For example, membrane hyperpolarization caused by KATP channel opening may have affected the activity of voltage-gated calcium channels, thereby indirectly influencing MMP, apoptosis and the PI3K/AKT signaling pathway. To unequivocally distinguish between the channel-dependent and independent functions of ABCC9, future studies should employ patch-clamp techniques (84) to directly measure KATP currents in cardiomyocytes following ABCC9 knockdown. Furthermore, gain-of-function and loss-of-function experiments using specific KATP channel openers, such as pinacidil, or inhibitors, such as glibenclamide, (85) are warranted. Such investigations would provide more robust support for the conclusions of the present study and offer a more comprehensive elucidation of the mechanistic role of ABCC9 in MH.

However, the present study had some limitations. First, although ABCC9 knockdown had a significant effect on the treatment of MH, it would be more convincing if the overexpression of ABCC9 was used to also obtain the corresponding results. Nevertheless, since protein expression is often subject to endogenous saturation, simple overexpression may not necessarily induce a hypertrophic phenotype, and loss-of-function approaches could potentially reveal the physiological role of ABCC9 more clearly. Furthermore, only the core proteins in the PI3K signaling pathway were evaluated in the present study, and the detailed molecular mechanisms of downstream regulation of PI3K/AKT signaling during MH have not been fully elucidated. Finally, the present study demonstrated that ABCC9 knockdown protected against pathological cardiac hypertrophy predominantly in ISO-induced AC16 cells; therefore, further evaluation of efficacy in animal models is needed. In future studies, the role of ABCC9 overexpression in MH pathogenesis should be investigated, the downstream molecular targets of the PI3K/AKT signaling pathway should be explored in greater detail and the therapeutic efficacy of ABCC9 knockdown or inhibition should be validated in animal models to fully establish its clinical relevance.

In summary, the present study demonstrated that ABCC9 knockdown alleviated ISO-induced MH partly by regulating the PI3K/AKT pathway, which subsequently improved mitochondrial function and thereby reduced myocardial apoptosis, attenuated oxidative stress and preserved cardiac function. The present study provides new evidence for the role of ABCC9 in MH pathogenesis, and ABCC9 can be regarded as a potential promising candidate target for clinical intervention.

Acknowledgements

Not applicable.

Funding

The present study was supported by the Shanghai Pudong New Area Health Commission (grant no. 2025-PWYC-14).

Availability of data and materials

The data generated in the present study may be requested from the corresponding author.

Authors' contributions

QP, RC, LM and YL contributed to the study conception and design. QP performed experiments, analyzed the data and wrote the manuscript. RC analyzed data and revised the manuscript. YL and LM supervised the work and analyzed data. YL and LM confirm the authenticity of all the raw data. All authors read and approved the final version of the manuscript.

Ethics approval and consent to participate

Not applicable.

Patient consent for publication

Not applicable.

Competing interests

The authors declare that they have no competing interests.

References

1. Jagannathan R, Patel SA, Ali MK and Narayan KMV: Global updates on cardiovascular disease mortality trends and attribution of traditional risk factors. Curr Diab Rep 19: 44, 2019.
2. Kahleova H, Levin S and Barnard ND: Vegetarian dietary patterns and cardiovascular disease. Prog Cardiovasc Dis 61: 54-61, 2018.
3. Tsao CW, Aday AW, Almarzooq ZI, Alonso A, Beaton AZ, Bittencourt MS, Boehme AK, Buxton AE, Carson AP, Commodore-Mensah Y, *et al*: Heart disease and stroke Statistics-2022 update: A report from the American heart association. Circulation 145: e153-e639, 2022.
4. Tan Y-Q, Chen HW and Li J: Astragaloside IV: An effective drug for the treatment of cardiovascular diseases. Drug Des Devel Ther 14: 3731-3746, 2020.
5. Roth GA, Mensah GA, Johnson CO, Addolorato G, Ammirati E, Baddour LM, Barengo NC, Beaton AZ, Benjamin EJ, Benziger CP, *et al*: Global burden of cardiovascular diseases and risk factors, 1990-2019. J Am Coll Cardiol 76: 2982-3021, 2020.
6. Zhu XY, Shi MQ, Jiang ZM, Xiao Li, Tian JW and Su FF: Global, regional, and national burden of cardiovascular diseases attributable to metabolic risks across all age groups from 1990 to 2021: An analysis of the 2021 global burden of disease study data. BMC Public Health 25: 1704, 2025.
7. Yan Z, Zhao W, Zhao N, Liu Y, Yang B, Wang L, Liu J, Wang D, Wang J, Jiao X, *et al*: PRMT1 alleviates isoprenaline-induced myocardial hypertrophy by methylating SRSF1. Acta Biochim Biophys Sin (Shanghai) 57: 1338-1349, 2024.
8. Chang CC, Cheng HC, Chou WC, Huang YT, Hsieh PL, Chu PM and Lee SD: Sesamin suppresses angiotensin-II-enhanced oxidative stress and hypertrophic markers in H9c2 cells. Environ Toxicol 38: 2165-2172, 2023.
9. Feng Z, Pan L, Qiao C, Yang Y, Yang X and Xie Y: Cardamonin intervenes in myocardial hypertrophy progression by regulating Usp18. Phytomedicine 134: 155970, 2024.
10. Pang Y, Wu L, Xia J, Xu X, Gao C, Hou L and Jiang L: Trim38 attenuates pressure overload-induced cardiac hypertrophy by suppressing the TAK1/JNK/P38 signaling pathway. Int J Mol Med 55: 98, 2025.
11. Li D, Guo Y, Cen X, Qiu HL, Chen S, Zeng XF, Zeng Q, Xu M and Tang QZ: Lupeol protects against cardiac hypertrophy via TLR4-PI3K-Akt-NF-κB pathways. Acta Pharmacol Sin 43: 1989-2002, 2022.
12. Oudit GY, Crackower MA, Eriksson U, Sarao R, Kozieradzki I, Sasaki T, Irie-Sasaki J, Gidrewicz D, Rybin VO, Wada T, *et al*: Phosphoinositide 3-kinase gamma-deficient mice are protected from isoproterenol-induced heart failure. Circulation 108: 2147-2152, 2003.
13. Zhou WW, Dai C, Liu WZ, Zhang C, Zhang Y, Yang GS, Guo QH, Li S, Yang HX and Li AY: *Gentianella acuta* improves TAC-induced cardiac remodelling by regulating the Notch and PI3K/Akt/FOXO1/3 pathways. Biomed Pharmacother 154: 113564, 2022.
14. Ghafouri-Fard S, Khanbabapour Sasi A, Hussen BM, Shoorei H, Siddiq A, Taheri M and Ayatollahi SA: Interplay between PI3K/AKT pathway and heart disorders. Mol Biol Rep 49: 9767-9781, 2022.
15. Li J, Yan C, Wang Y, Chen C, Yu H, Liu D, Huang K and Han Y: GCN5-mediated regulation of pathological cardiac hypertrophy via activation of the TAK1-JNK/p38 signaling pathway. Cell Death Dis 13: 421, 2022.
16. Zhang T, Li L, Mo X, Xie S, Liu S, Zhao N, Zhang H, Chen S, Zeng X, Wang S, *et al*: Matairesinol blunts adverse cardiac remodeling and heart failure induced by pressure overload by regulating Prdx1 and PI3K/AKT/FOXO1 signaling. Phytomedicine 135: 156054, 2024.
17. Liu Z, Liu H and Wang J: Astragaloside IV protects against the pathological cardiac hypertrophy in mice. Biomed Pharmacother 97: 1468-1478, 2018.
18. Qian W, Yu D, Zhang J, Hu Q, Tang C, Liu P, Ye P, Wang X, Lv Q, Chen M and Sheng L: Wogonin attenuates isoprenaline-induced myocardial hypertrophy in mice by suppressing the PI3K/Akt pathway. Front Pharmacol 9: 896, 2018.
19. Solbach TF, König J, Fromm MF and Zolk O: ATP-binding cassette transporters in the heart. Trends Cardiovasc Med 16: 7-15, 2006.
20. Park S, Lim BBC, Perez-Terzic C, Mer G and Terzic A: Interaction of asymmetric ABCC9-encoded nucleotide binding domains determines KATP channel SUR2A catalytic activity. J Proteome Res 7: 1721-1728, 2008.
21. Aubert G, Barefield DY, Demonbreun AR, Ramratnam M, Fallon KS, Warner JL, Rossi AE, Hadhazy M, Makielski JC and McNally EM: Deletion of sulfonylurea receptor 2 in the adult myocardium enhances cardiac glucose uptake and is cardioprotective. JACC Basic Transl Sci 4: 251-268, 2019.
22. Flagg TP, Kurata HT, Masia R, Caputa G, Magnuson MA, Lefer DJ, Coetzee WA and Nichols CG: Differential structure of atrial and ventricular KATP: Atrial KATP channels require SUR1. Circ Res 103: 1458-1465, 2008.
23. Stoller D, Kakkar R, Smelley M, Chalupsky K, Earley JU, Shi NQ, Makielski JC and McNally EM: Mice lacking sulfonylurea receptor 2 (SUR2) ATP-sensitive potassium channels are resistant to acute cardiovascular stress. J Mol Cell Cardiol 43: 445-454, 2007.
24. Fahrenbach JP, Stoller D, Kim G, Aggarwal N, Yerokun B, Earley JU, Hadhazy M, Shi NQ, Makielski JC and McNally EM: Abcc9 is required for the transition to oxidative metabolism in the newborn heart. FASEB J 28: 2804-2815, 2014.
25. Mohammed Abdul KS, Jovanović S, Du Q, Sukhodub A and Jovanović A: A link between ATP and SUR2A: A novel mechanism explaining cardioprotection at high altitude. Int J Cardiol 189: 73-76, 2015.
26. McClenaghan C and Nichols CG: Kir6.1 and SUR2B in Cantú syndrome. Am J Physiol Cell Physiol 323: C920-C935, 2022.
27. McClenaghan C, Huang Y, Yan Z, Harter TM, Halabi CM, Chalk R, Kovacs A, van Haaften G, Remedi MS and Nichols CG: Glibenclamide reverses cardiovascular abnormalities of Cantu syndrome driven by KATP channel overactivity. J Clin Invest 130: 1116-1121, 2020.
28. McClenaghan C, Huang Y, Matkovich SJ, Kovacs A, Weinheimer CJ, Perez R, Broekelmann TJ, Harter TM, Lee JM, Remedi MS and Nichols CG: The mechanism of High-output cardiac hypertrophy arising from potassium channel Gain-of-Function in Cantú syndrome. Function (Oxf) 1: zqaa004, 2020.
29. Zhang H, Hanson A, de Almeida TS, Emfinger C, McClenaghan C, Harter T, Yan Z, Cooper PE, Brown GS, Arakel EC, *et al*: Complex consequences of Cantu syndrome SUR2 variant R1154Q in genetically modified mice. JCI Insight 6: e145934, 2021.
30. Fernlund E, Kissopoulou A, Green H, Karlsson JE, Ellegård R, Årstrand HK, Jonasson J and Gunnarsson C: Hereditary hypertrophic cardiomyopathy in children and young Adults-the value of reevaluating and expanding gene panel analyses. Genes (Basel) 11: 1472, 2020.
31. Livak KJ and Schmittgen TD: Analysis of relative gene expression data using real-time quantitative PCR and the 2(-Delta Delta C(T)) method. Methods 25: 402-408, 2001.

32. He K, Wang X, Li T, Li Y and Ma L: Chlorogenic acid attenuates isoproterenol Hydrochloride-induced cardiac hypertrophy in AC16 cells by inhibiting the Wnt/β-Catenin signaling pathway. Molecules 29: 760, 2024.
33. Wang X, He K, Ma L, Wu L, Yang Y and Li Y: Puerarin attenuates isoproterenol-induced myocardial hypertrophy via inhibition of the Wnt/β-catenin signaling pathway. Mol Med Rep 26: 306, 2022.
34. Dorn GW and Force T: Protein kinase cascades in the regulation of cardiac hypertrophy. J Clin Invest 115: 527-537, 2005.
35. Bisserier M, Berthouze-Duquesnes M, Breckler M, Tortosa F, Fazal L, de Régibus A, Laurent AC, Varin A, Lucas A, Branchereau M, *et al*: Carabin protects against cardiac hypertrophy by blocking calcineurin, Ras, and Ca2+/calmodulin-dependent protein kinase II signaling. Circulation 131: 390-400, 2015.
36. de Lucia C, Eguchi A and Koch WJ: New Insights in cardiac β-adrenergic signaling during heart failure and aging. Front Pharmacol 9: 904, 2018.
37. Jeong MY, Lin YH, Wennersten SA, Demos-Davies KM, Cavasin MA, Mahaffey JH, Monzani V, Saripalli C, Mascagni P, Reece TB, *et al*: Histone deacetylase activity governs diastolic dysfunction through a nongenomic mechanism. Sci Transl Med 10: eaao0144, 2018.
38. Singh K, Xiao L, Remondino A, Sawyer DB and Colucci WS: Adrenergic regulation of cardiac myocyte apoptosis. J Cell Physiol 189: 257-265, 2001.
39. Lymperopoulos A, Rengo G and Koch WJ: Adrenergic nervous system in heart failure: Pathophysiology and therapy. Circ Res 113: 739-753, 2013.
40. Su H, Liu M, Wang S, Tian B, Hu H, Ma LK and Pan J: Co-administration of isoprenaline and phenylephrine induced a new HFrEF mouse model through activation of both SNS and RAAS. Front Cardiovasc Med 12: 1531509, 2025.
41. Ferrari R, Ceconi C, Curello S and Visioli O: The neuroendocrine and sympathetic nervous system in congestive heart failure. Eur Heart J 19 (Suppl F): F45-F51, 1998.
42. Abi-Gerges A, Castro L, Leroy J, Domergue V, Fischmeister R and Vandecasteele G: Selective changes in cytosolic β-adrenergic cAMP signals and L-type Calcium Channel regulation by Phosphodiesterases during cardiac hypertrophy. J Mol Cell Cardiol 150: 109-121, 2021.
43. Xu H, Wang Z, Chen M, Zhao W, Tao T, Ma L, Ni Y and Li W: YTHDF2 alleviates cardiac hypertrophy via regulating Myh7 mRNA decoy. Cell Biosci 11: 132, 2021.
44. Murray DR, Prabhu SD and Chandrasekar B: Chronic beta-adrenergic stimulation induces myocardial proinflammatory cytokine expression. Circulation 101: 2338-2341, 2000.
45. Liu BY, Li L, Liu GL, Ding W, Chang WG, Xu T, Ji XY, Zheng XX, Zhang J and Wang JX: Baicalein attenuates cardiac hypertrophy in mice via suppressing oxidative stress and activating autophagy in cardiomyocytes. Acta Pharmacol Sin 42: 701-714, 2021.
46. Wei H, Guo X, Yan J, Tian X, Yang W, Cui K, Wang L and Bingyan G: Neuregulin-4 alleviates isoproterenol (ISO)-induced cardial remodeling by inhibiting inflammation and apoptosis via AMPK/NF-κB pathway. Int Immunopharmacol 143: 113301, 2024.
47. Yang J, Wang Z and Chen DL: Shikonin ameliorates isoproterenol (ISO)-induced myocardial damage through suppressing fibrosis, inflammation, apoptosis and ER stress. Biomed Pharmacother 93: 1343-1357, 2017.
48. Yang D, Liu HQ, Liu FY, Guo Z, An P, Wang MY, Yang Z, Fan D and Tang QZ: Mitochondria in pathological cardiac hypertrophy research and therapy. Front Cardiovasc Med 8: 822969, 2022.
49. Singh GK, McClenaghan C, Aggarwal M, Gu H, Remedi MS, Grange DK and Nichols CG: A unique High-output cardiac hypertrophy phenotype arising from low systemic vascular resistance in cantu syndrome. J Am Heart Assoc 11: e027363, 2022.
50. Samad M, Malempati S and Restini CBA: Natriuretic peptides as biomarkers: Narrative review and considerations in cardiovascular and respiratory dysfunctions. Yale J Biol Med 96: 137-149, 2023.
51. Edwards JG: Cardiac MHC gene expression: More complexity and a step forward. Am J Physiol Heart Circ Physiol 294: H14-H15, 2008.
52. Xu J, Sun Z, Li J, Li J, Li Y, Huang H, Yuan F, Liu M and Fang Z: Qian Yang Yu Yin Granule prevents hypertensive cardiac remodeling by inhibiting NLRP3 inflammasome activation via Nrf2. J Ethnopharmacol 337: 118820, 2025.
53. Nakamura M and Sadoshima J: Mechanisms of physiological and pathological cardiac hypertrophy. Nat Rev Cardiol 15: 387-407, 2018.
54. Münzel T, Camici GG, Maack C, Bonetti NR, Fuster V and Kovacic JC: Impact of oxidative stress on the heart and vasculature: Part 2 of a 3-Part series. J Am Coll Cardiol 70: 212-229, 2017.
55. Fandy TE, Jiemjit A, Thakar M, Rhoden P, Suarez L and Gore SD: Decitabine induces delayed reactive oxygen species (ROS) accumulation in leukemia cells and induces the expression of ROS generating enzymes. Clin Cancer Res 20: 1249-1258, 2014.
56. Dai DF, Johnson SC, Villarin JJ, Chin MT, Nieves-Cintrón M, Chen T, Marcinek DJ, Dorn GW II, Kang YJ, Prolla TA, *et al*: Mitochondrial oxidative stress mediates angiotensin II-induced cardiac hypertrophy and Galphaq overexpression-induced heart failure. Circ Res 108: 837-846, 2011.
57. Qi B, Xu R, Jin Y, Wang Y, Cheng T, Liu C, Ji Y, Guo L, Li J, Gao Y, *et al*: A critical role for IL-21/IL-21 receptor signaling in isoproterenol-induced cardiac remodeling. Sci Rep 15: 18985, 2025.
58. Mustafa M, Ahmad R, Tantry IQ, Ahmad W, Siddiqui S, Alam M, Abbas K, Moinuddin, Hassan MI, Habib S and Islam S: Apoptosis: A comprehensive overview of signaling pathways, morphological changes, and physiological significance and therapeutic implications. Cells 13: 1838, 2024.
59. Cao H, Zhao L, Yuan Y, Liao C, Zeng W, Li A, Huang Q, Zhao Y, Fan Y, Jiang L, *et al*: Lipoamide attenuates hypertensive myocardial hypertrophy through PI3K/Akt-mediated Nrf2 signaling pathway. J Cardiovasc Transl Res 17: 910-922, 2024.
60. Mei L, Chen Y, Chen P, Chen H, He S, Jin C, Wang Y, Hu Z, Li W, Jin L, *et al*: Fibroblast growth factor 7 alleviates myocardial infarction by improving oxidative stress via PI3Kα/AKT-mediated regulation of Nrf2 and HXK2. Redox Biol 56: 102468, 2022.
61. Maruyama N, Ogata T, Kasahara T, Hamaoka T, Higuchi Y, Tsuji Y, Tomita S, Sakamoto A, Nakanishi N and Matoba S: Loss of Cavin-2 destabilizes phosphatase and tensin homologue and enhances Akt signalling pathway in cardiomyocytes. Cardiovasc Res 120: 1562-1576, 2024.
62. Zhang Q, Luo Y, Zheng Q, Zhao H, Wei X and Li X: Itaconate attenuates autoimmune hepatitis via PI3K/AKT/mTOR pathway-mediated inhibition of dendritic cell maturation and autophagy. Heliyon 9: e17551, 2023.
63. Vainio L, Taponen S, Kinnunen SM, Halmetoja E, Szabo Z, Alakoski T, Ulvila J, Junttila J, Lakkisto P, Magga J and Kerkelä R: GSK3β serine 389 phosphorylation modulates cardiomyocyte hypertrophy and ischemic injury. Int J Mol Sci 22: 13586, 2021.
64. Heineke J and Molkentin JD: Regulation of cardiac hypertrophy by intracellular signalling pathways. Nat Rev Mol Cell Biol 7: 589-600, 2006.
65. Gu J, Qiu M, Lu Y, Ji Y, Qian Z and Sun W: Piperlongumine attenuates angiotensin-II-induced cardiac hypertrophy and fibrosis by inhibiting Akt-FoxO1 signalling. Phytomedicine 82: 153461, 2021.
66. Ren J, Yang L, Zhu L, Xu X, Ceylan AF, Guo W, Yang J and Zhang Y: Akt2 ablation prolongs life span and improves myocardial contractile function with adaptive cardiac remodeling: Role of Sirt1-mediated autophagy regulation. Aging Cell 16: 976-987, 2017.
67. Bencun M, Spreyer L, Boileau E, Eschenbach J, Frey N, Dieterich C and Völkers M: A novel uORF regulates folliculin to promote cell growth and lysosomal biogenesis during cardiac stress. Sci Rep 15: 3319, 2025.
68. Völkers M, Toko H, Doroudgar S, Din S, Quijada P, Joyo AY, Ornelas L, Joyo E, Thuerauf DJ, Konstandin MH, *et al*: Pathological hypertrophy amelioration by PRAS40-mediated inhibition of mTORC1. Proc Natl Acad Sci USA 110: 12661-12666, 2013.
69. Liu Q, Chen Y, Auger-Messier M and Molkentin JD: Interaction between NFκB and NFAT coordinates cardiac hypertrophy and pathological remodeling. Circ Res 110: 1077-1086, 2012.
70. Yu H, Lin L, Zhang Z, Zhang H and Hu H: Targeting NF-κB pathway for the therapy of diseases: Mechanism and clinical study. Signal Transduct Target Ther 5: 209, 2020.
71. Czabotar PE, Lessene G, Strasser A and Adams JM: Control of apoptosis by the BCL-2 protein family: Implications for physiology and therapy. Nat Rev Mol Cell Biol 15: 49-63, 2014.
72. Meng X, Cui J and He G: Bcl-2 is involved in cardiac hypertrophy through PI3K-Akt pathway. Biomed Res Int 2021: 6615502, 2021.
73. Condorelli G, Drusco A, Stassi G, Bellacosa A, Roncarati R, Iaccarino G, Russo MA, Gu Y, Dalton N, Chung C, *et al*: Akt induces enhanced myocardial contractility and cell size in vivo in transgenic mice. Proc Natl Acad Sci USA 99: 12333-12338, 2002.

74. Schiekofer S, Shiojima I, Sato K, Galasso G, Oshima Y and Walsh K: Microarray analysis of Akt1 activation in transgenic mouse hearts reveals transcript expression profiles associated with compensatory hypertrophy and failure. Physiol Genomics 27: 156-170, 2006.
75. Matsui T, Li L, Wu JC, Cook SA, Nagoshi T, Picard MH, Liao R and Rosenzweig A: Phenotypic spectrum caused by transgenic overexpression of activated Akt in the heart. J Biol Chem 277: 22896-22901, 2002.
76. Zhang T, Xiu YH, Xue H, Li YN, Cao JL, Hou WS, Liu J, Cui YH, Xu T, Wang Y and Jin CH: A mechanism of Isoorientin-induced apoptosis and migration inhibition in gastric cancer AGS cells. Pharmaceuticals (Basel) 15: 1541, 2022.
77. Marchi S, Giorgi C, Suski JM, Agnoletto C, Bononi A, Bonora M, De Marchi E, Missiroli S, Patergnani S, Poletti F, *et al*: Mitochondria-Ros crosstalk in the control of cell death and aging. J Signal Transduct 2012: 329635, 2012.
78. Manning BD and Toker A: AKT/PKB Signaling: Navigating the network. Cell 169: 381-405, 2017.
79. Nagoshi T, Matsui T, Aoyama T, Leri A, Anversa P, Li L, Ogawa W, del Monte F, Gwathmey JK, Grazette L, *et al*: PI3K rescues the detrimental effects of chronic Akt activation in the heart during ischemia/reperfusion injury. J Clin Invest 115: 2128-2138, 2005.
80. Derossi D, Williams EJ, Green PJ, Dunican DJ and Doherty P: Stimulation of mitogenesis by a cell-permeable PI 3-kinase binding peptide. Biochem Biophys Res Commun 251: 148-152, 1998.
81. Bryan J, Muñoz A, Zhang X, Düfer M, Drews G, Krippeit-Drews P and Aguilar-Bryan L: ABCC8 and ABCC9: ABC transporters that regulate K+ channels. Pflugers Arch 453: 703-718, 2007.
82. Seino S: ATP-sensitive potassium channels: A model of heteromultimeric potassium channel/receptor assemblies. Annu Rev Physiol 61: 337-362, 1999.
83. Huang Y, McClenaghan C, Harter TM, Hinman K, Halabi CM, Matkovich SJ, Zhang H, Brown GS, Mecham RP, England SK, *et al*: Cardiovascular consequences of KATP overactivity in Cantu syndrome. JCI Insight 3: e121153, 2018.
84. Li K, Janve VS and Denton JS: Automated patch clamp analysis of heterologously expressed Kir6.2/SUR1 and Kir6.1/SUR2B KATP currents. Am J Physiol Cell Physiol 329: C82-C92, 2025.
85. Winter A, Nepper P, Hermann M, Bayer F, Riess S, Salem R, Hlavicka J, Prinzing A, Hecker F, Holubec T, *et al*: Glibenclamide serves as a potent vasopressor to treat vasoplegia after cardiopulmonary bypass and reperfusion in a porcine model. Int J Mol Sci 26: 4040, 2025.